ARTICLE OPEN

Check for updates

# AAV-mediated expression of a new conformational anti-aggregated α-synuclein antibody prolongs survival in a genetic model of α-synucleinopathies

Matthias Düchs[1], Dragica Blazevic[1], Philipp Rechtsteiner[1], Cynthia Kenny[2], Thorsten Lamla[1], Sarah Low[2], Jimmy Savistchenko[3], Manuela Neumann[4,5], Ronald Melki[3], Tanja Schönberger[1], Birgit Stierstorfer[1], David Wyatt[1], Frederik Igney[1] and Thomas Ciossek[1]✉

Prion-like transmission of pathology in α-synucleinopathies like Parkinson's disease or multiple system atrophy is increasingly recognized as one potential mechanism to address disease progression. Active and passive immunotherapies targeting insoluble, aggregated α-synuclein are already being actively explored in the clinic with mixed outcomes so far. Here, we report the identification of 306C7B3, a highly selective, aggregate-specific α-synuclein antibody with picomolar affinity devoid of binding to the monomeric, physiologic protein. 306C7B3 binding is Ser129-phosphorylation independent and shows high affinity to several different aggregated α-synuclein polymorphs, increasing the likelihood that it can also bind to the pathological seeds assumed to drive disease progression in patients. In support of this, highly selective binding to pathological aggregates in postmortem brains of MSA patients was demonstrated, with no staining in samples from other human neurodegenerative diseases. To achieve CNS exposure of 306C7B3, an adeno-associated virus (AAV) based approach driving expression of the secreted antibody within the brain of (Thy-1)-[A30P]-hα-synuclein mice was used. Widespread central transduction after intrastriatal inoculation was ensured by using the AAV2HBKO serotype, with transduction being spread to areas far away from the inoculation site. Treatment of (Thy-1)-[A30P]-hα-synuclein mice at the age of 12 months demonstrated significantly increased survival, with 306C7B3 concentration reaching 3.9 nM in the cerebrospinal fluid. These results suggest that AAV-mediated expression of 306C7B3, targeting extracellular, presumably disease-propagating aggregates of α-synuclein, has great potential as a disease-modifying therapy for α-synucleinopathies as it ensures CNS exposure of the antibody, thereby mitigating the selective permeability of the blood-brain barrier.

*npj Parkinson's Disease* (2023)9:91 ; https://doi.org/10.1038/s41531-023-00542-9

## INTRODUCTION

α-synucleinopathies, like Parkinson's disease (PD), dementia with Lewy bodies (DLB) and multiple system atrophy (MSA), are relentless neurodegenerative diseases with no disease-modifying therapies for patients available to date. These diseases are characterized by intracellular deposits rich in an aggregated form of the 140 amino acid residue-long, intrinsically disordered protein α-synuclein[1,2]. These deposits are known as Lewy bodies, Lewy neurites or oligodendroglial cytoplasmic inclusions and are regarded as histological hallmarks allowing definite classification of these diseases[3,4], although exceptions exist for some rare familiar cases (reviewed in ref. [5]). α-synuclein had first been linked to PD based on the identification of a pathogenic mutation[6] and since been confirmed to be genetically linked to PD based on additional point mutations as well as gene duplications and triplications causing highly penetrant autosomal forms of PD[7,8]. These familial point mutations as well as increased gene dosage of wildtype α-synuclein usually cause an early onset of disease combined with rapid disease progression. Overall incidence of mutation carriers is low, but genome wide association studies (GWAS) demonstrated an association between α-synuclein and the risk of developing disease even for idiopathic PD cases[9], with the association toward the SNCA gene coding for α-synuclein representing the strongest signal in PD GWAS studies identified so far[10].

The physiological function of α-synuclein is still poorly understood. The protein is highly enriched in presynaptic nerve terminals[11]. It has been suggested to play a role in presynaptic function[12], and has been shown to allow SNARE complex assembly, a key component for membrane fusion between vesicles and presynaptic terminals during neurotransmission[13]. However, genetic models with loss of α-synuclein expression present with only minor deficits[14–16]. α-Synuclein aggregation leads to the loss of function of its physiological role[17], but also to a gain of pathological function at the origin of PD, DLB or MSA. Recent work in experimental systems support the spread of misfolded, aggregated α-synuclein between neuronal cells[18–21], potentially explaining the observed temporal and spatial progression of disease in affected patients[22], and the presence of Lewy bodies in juvenile grafts within the brain of PD patiens[23,24]. These models assume that fibrillar α-synuclein is either secreted or passively released from neurons carrying intracellular aggregations, which spreads within the brain and—upon uptake—seeds the aggregation of endogenous α-synuclein in recipient neurons in a prion-like manner (reviewed in ref. [25]). An important element of this model is the fact that such seeds can be detected within

[1]Boehringer Ingelheim Pharma GmbH & Co KG, Biberach an der Riss, Germany. [2]Boehringer Ingelheim USA, Ridgefield, CT, USA. [3]Institut Francois Jacob (MIRCen), CEA, CNRS, Fontenay-aux-Roses, France. [4]Molecular Neuropathology of Neurodegenerative Diseases, German Center for Neurodegenerative Diseases, Tübingen, Germany. [5]Department of Neuropathology, University Hospital of Tübingen, Tübingen, Germany. ✉email: thomas.ciossek@boehringer-ingelheim.com

cerebrospinal fluid (CSF) samples from patients[26–28], although the exact structural composition of these seeds has so far not been elucidated.

A potential prion-like cell-to-cell transmission of pathological aggregates of α-synuclein enabled the therapeutic concept of antibody-mediated blockage of disease progression in PD, DLB and MSA. This concept has been tested preclinically as well as clinically (summarized in ref. [29]), with mixed results, especially regarding beneficial effects in patients. Challenges to be considered in the clinical application of this concept include the problem of sufficient delivery of antibodies to the human brain (serum to plasma ratio of about 1:440; ref. [30]), especially since the blood-brain barrier seems to be only mildly perturbed in PD or MSA patients (refs. [31,32], see also actual exposure data in refs. [33,34]). In addition, some of the advanced immunotherapies (PRX002, ref. [33]; PDE03A, ref. [35]) utilize antibodies with significant binding affinity toward non-aggregated, monomeric α-synuclein, a property that might be considered undesirable considering the high plasma exposure measurable in man[36,37]. This potentially blocks the antigen binding site of these antibodies upon intravenous administration into patients as exemplified by the strong reduction in plasma α-synuclein upon PRX002 treatment[38].

Herein, we describe the identification and characterization of a new anti-α-synuclein antibody directed against the aggregated form of the protein that was counter-selected against monomeric α-synuclein. We detected sensitive and specific binding of our antibody to α-synuclein aggregates in post-mortem human brain tissue. Furthermore, the therapeutic efficacy of 306C7B3, targeting extracellular, presumably disease-propagating α-synuclein aggregates, was analyzed in a murine disease model with age-dependent development of pathology, based upon Adeno-Associated Virus (AAV) mediated antibody expression ensuring high central antibody exposure.

## RESULTS

### Hybridoma screening for aggregate specific anti-human α-synuclein antibodies

Bacterially expressed and highly purified human α-synuclein was aggregated in vitro to pre-formed fibrillar α-synuclein (PFF), based upon established methods[39]. Care was taken to confirm biological activity of the obtained preparations by characterization in an SH-SY5Y based cellular assay, in which their potential to drive intracellular aggregation of human α-synuclein is measured by the appearance of mesh-like, pSer129-positive human α-synuclein aggregates. Active preparations underwent further biophysical purification to deplete monomeric α-synuclein. Mice were repeatedly immunized with these aggregated preparations of human α-synuclein and isolated hybridomas screened for clones with high binding activity toward aggregated α-synuclein, combined with low to no binding to monomeric human α-synuclein. Selected clones were further characterized as depicted in Supplementary Fig. 1, initially also including an analysis of their capacity to block intracellular aggregation of α-synuclein in a mouse primary neuron assay (not pursued at later stages, see Supplementary Fig. 3).

### Characterization of 306B7C3

As shown in Fig. 1a (left panel), the hybridoma clone 306C7B3 was finally selected based on its strong and almost irreversible binding to aggregated human α-synuclein with a calculated $K_D$ of 15 pM and a $k_{off}$ of less than $10^{-5}$/s, as determined in a surface plasmon resonance assay. Importantly, no binding to monomeric human α-synuclein could be measured (Fig. 1a, right panel). 306C7B3 was further characterized for its functional activity regarding seeding of endogenous α-synuclein (aggregation indicated by Ser129 phosphorylation) in the above-described cellular assay (Fig. 1c). Prior to electroporation of the SH-SY5Y cells overexpressing A53T-mutated human α-synuclein, the antibody was pre-incubated with a large molar excess of monomeric human α-synuclein to fully block monomer-binding ability, followed by the addition of pre-formed fibrillar α-synuclein as seeds for intracellular aggregation (assay adapted from ref. [40]). 306C7B3, purified from its hybridoma supernatant, showed strong dose-dependent blockage of intracellular α-synuclein aggregation as analyzed by high content analysis of pSer129-positive intracellular aggregates (Fig. 1d, "hybridoma"). The primary amino acid sequence of 306C7B3 was determined by sequencing the hybridoma clone and 306C7B3 converted to a single-chain antibody (scIgG) by joining the light and heavy antibody chains with a covalent linker as shown in Supplementary Fig. 2a. This allowed the expression of 306C7B3 from a single open reading frame (scIgG-306C7B3). This construct, purified from HEK293 cells transiently transfected with the corresponding expression construct (similar to the one shown in Supplementary Fig. 2c but carrying an ubiquitous CMV promoter instead of the depicted neuron-specific human synapsin promoter), is as active as the 306C7B3 purified from the hybridoma (Fig. 1d, "scIgG").

### Epitope mapping of 306C7B3

The epitope of 306C7B3 was determined via PEPperMAP epitope mapping as shown in Fig. 2a. Control antibodies like Syn-1 (Fig. 2b) showed strong and sharp signals at an antibody concentration of 1 µg/ml, with similar data obtained for e.g., 9E4 (ref. [41], data not shown). However, no such staining could be observed with 306C7B3 at this antibody concentration. Only by raising the antibody concentration tenfold (Fig. 2, red line), a broad area of 306C7B3 binding to C-terminal human α-synuclein 15-mer peptides could be observed, defining its epitope ("YQDYEPE", amino acids 133–139; as calculated based upon the individual binding intensities to the 15mer α-synuclein peptides). This, together with the absence of binding to monomer (Fig. 1a), suggests that 306C7B3 rather recognizes a conformational epitope human α-synuclein adopts within PFFs, and not to a linear amino acid epitope.

### 306C7B3 binding to structurally distinct human α-synuclein assemblies

306C7B3 was identified by using human α-synuclein PFFs aggregated in a buffer at physiological pH as used for many in vitro as well as in vivo studies[18,39]. The extent to which 306C7B3 binds to structurally well characterized pure fibrillar and oligomeric α-synuclein polymorphs was assessed by filter trap measurements. Increasing amounts of the fibrillar polymorphs fibrils and ribbons[40], fibrils 65 and fibrils 91[42], fibrils 110[43], on fibrillar assembly pathway oligomers as well as dopamine or glutaraldehyde stabilized oligomers[44] were spotted on nitrocellulose membrane and the binding of 306C7B3 quantified (Fig. 3). 306C7B3 bound to all tested assemblies except fibrils 110, consistent with the absence of the α-synuclein C-terminal amino acid residues in fibrils 110. 306C7B3 barely bound to monomeric human α-synuclein. Finally, decreased binding was observed to dopamine or glutaraldehyde stabilized oligomers.

One of the most prominent post-translational modifications affecting α-synuclein in patient brains and in in vitro and in vivo models is the phosphorylation of Ser129. This residue lies close to the epitope of 306C7B3 as determined in the PEPperMAP epitope assessment and may interfere with 306C7B3 binding. A surface plasmon resonance assay comparing binding of 306C7B3 to non-phosphorylated as well as Ser129-phosphorylated, aggregated human α-synuclein showed that Ser129 phosphorylation does not affect 306C7B3 binding (Fig. 1b).

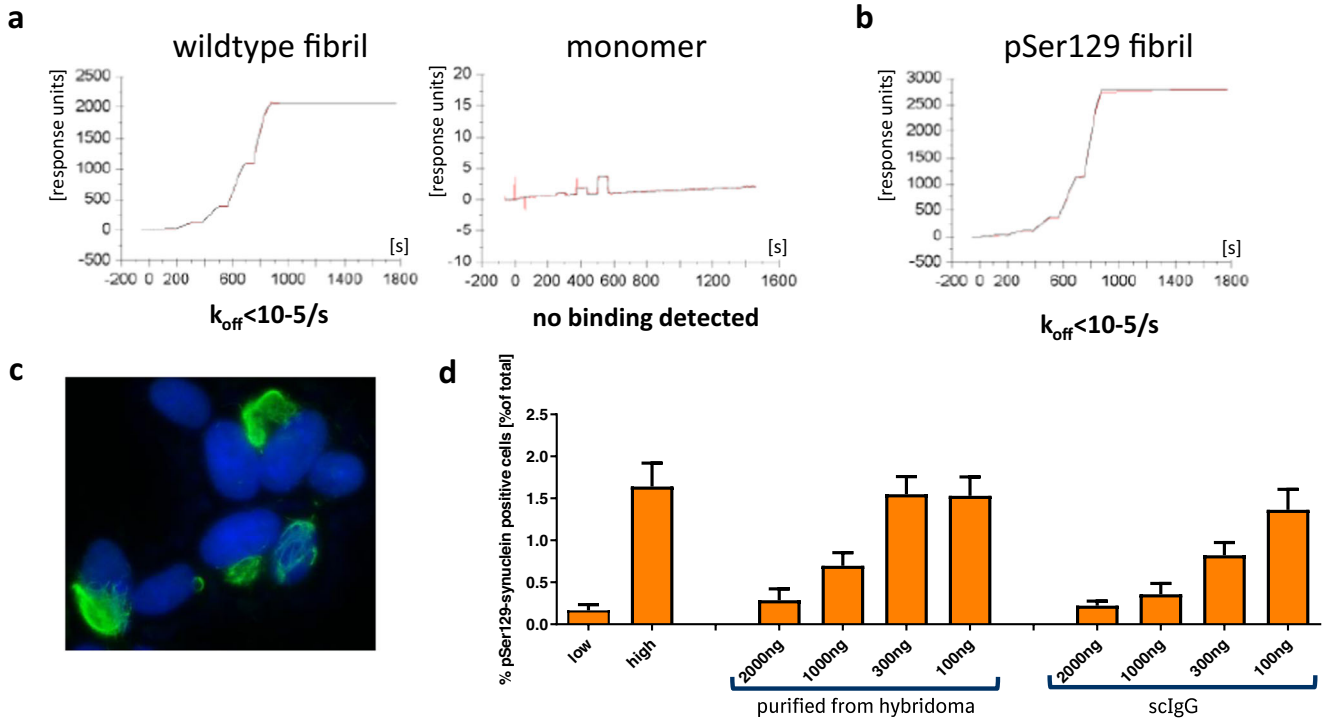


**Fig. 1 In vitro characterization of 306C7B3. a** Surface plasmon based affinity determination of 306C7B3 for fibrillar human α-synuclein (left) as well as for monomeric human α-synuclein (right). **b** Similar measurement as in (**a**), but using in vitro Ser129-phosphorylasted fibrillar human α-synuclein for the affinity determination. **c** Immunofluorescence staining of SH-SY5Y cells stably overexpressing A53T-mutated α-synuclein 2 days after electroporation with fibrillar α-synuclein. Intracellular mesh-like aggregates of pSer129 positive α-synuclein (green, Epitomics pSer129 antibody) are used for quantitative determination of functional activity of anti-α-synuclein antibodies (blue: DAPI staining). **d** Functional characterization of 306C7B3. Increasing amounts of purified antibody derived either from the original hybridoma clone or from a scIgG-based expression construct were preincubated with an excess of monomeric human α-synuclein, followed by addition of PFF α-synuclein and electroporation into SH-SY5Y cells stably overexpressing human A53T α-synuclein. High content-based analysis of cells stained for pSer129-positive intracellular aggregates demonstrates efficient inhibition of intracellular seeding by IgG-306C7B3 purified from the original hybridoma clone as well as single-chain IgG 306C7B3 (scIgG) derived from an expression construct. Error bars: standard deviation (s.d.).

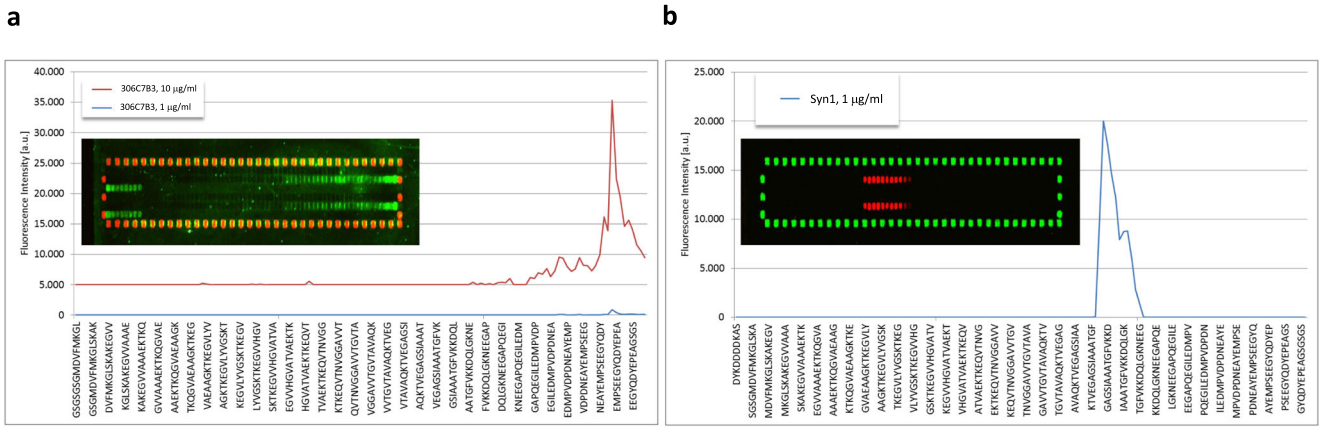


**Fig. 2 PEPperMAP epitope mapping. a** Either 1 µg/ml (blue line) or 10 µg/ml (red line) of IgG 306C7B3 were incubated with membranes spotted with 140 different 15mer peptides (each peptide printed in duplicate to be present in the top and bottom part of the array), representing the full human α-synuclein sequence with each peptide having a 14 amino acid overlap with the preceding peptide with the human α-synuclein sequence being elongated by neutral GSGSGSG linkers to avoid truncated peptides. Inset shows microarray stained with 10 µg/ml 306C7B3 (green: 306C7B3 signal, red: HA signal). Outer spots correspond to control peptides used to orient the microarray. Some cross-reactivity against the control peptides is observed for 306C7B3 at this high antibody concentration. Figure shows signal intensity obtained for individual peptide spots, identifying the epitope of 306C7B3 as being "YQDYEPE" (amino acids 133–139 of full-length human α-synuclein) located in the C-terminus of α-synuclein with overall low binding intensity toward the microarray spotted α-synuclein peptides. **b** Similar approach to determine the epitope of Syn1 at a concentration of 1 µg/ml (blue line, red: Syn1 signal, green: HA signal), identifying the epitope of Syn1 as being "AATGFVKK" (amino acids 90–97 of full-length human α-synuclein). Note that the exemplified peptide sequences do not reflect all tested 15mer peptides for better visualization—identical peptide arrays were used for the analysis of the different antibodies.

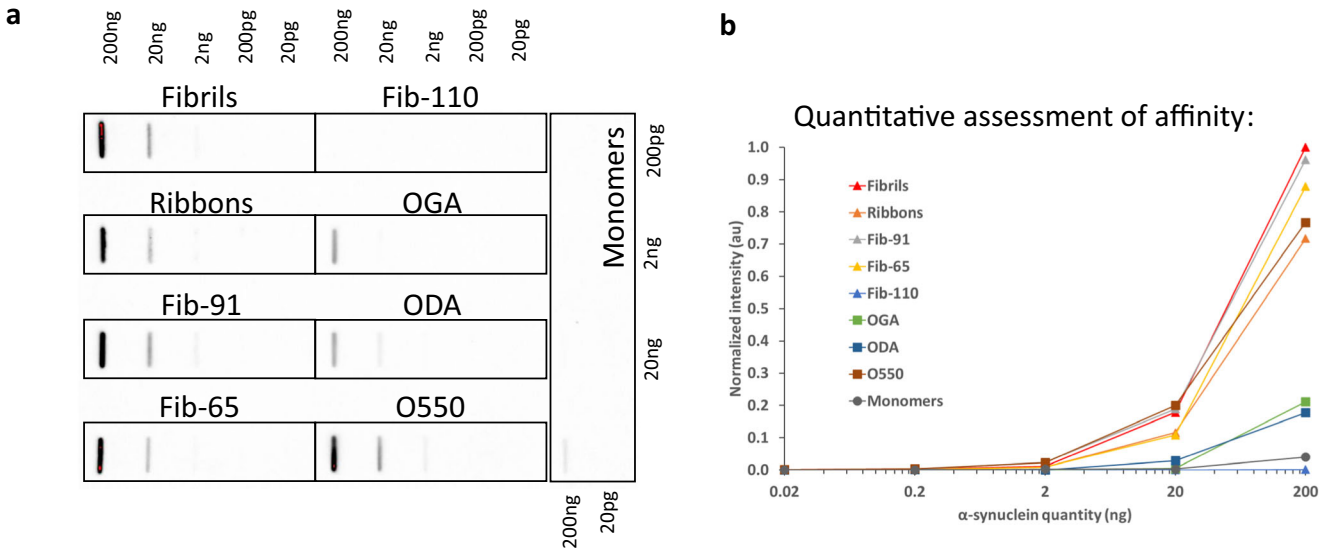


**Fig. 3 Filter trap assessment of 306C7B3 binding toward different in vitro generated assemblies of human α-synuclein.** Fibrils, ribbons, fibrils 65, fibrils 91, fibrils 110, on fibrillar assembly pathway oligomers (O550), dopamine stabilized (ODA) and glutaraldehyde stabilized (OGA) oligomers were spotted in increasing amounts on nitrocellulose filters and tested with 306C7B3. **a** Images obtained after ECL based visualization. **b** Quantification of signals using a Chemidoc MP imaging system. Blots derive from the same experiment and were processed in parallel.

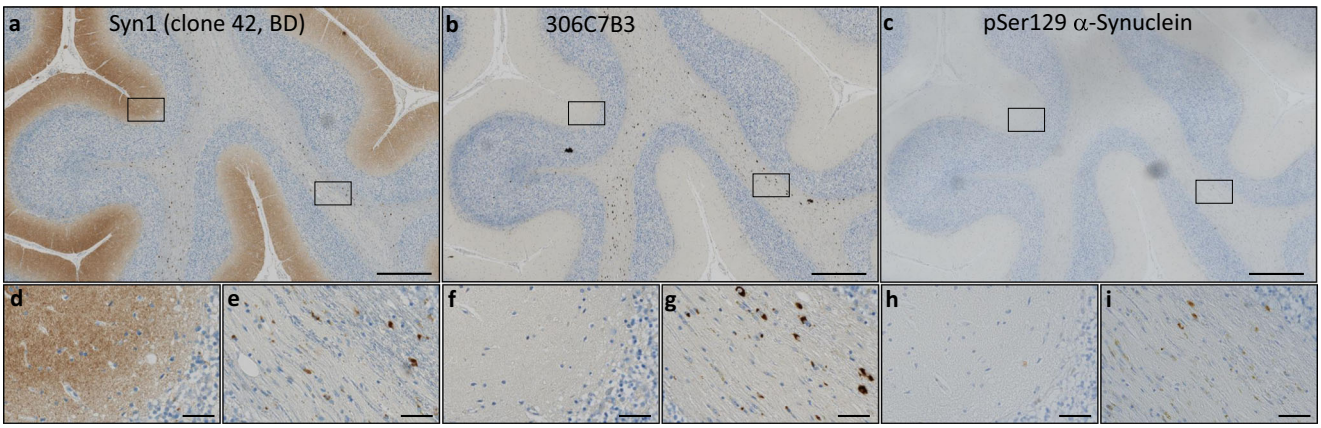


**Fig. 4 Immunohistochemical staining of adjacent sections of cerebellar tissue derived from a patient with multiple system atrophy (age at death 74 years, Braak&Braak stage I–II). a** Staining performed with the Syn1 antibody detecting monomeric α-synuclein in the molecular layer as well as aggregated forms of α-synuclein in the white matter fiber tracts. **b** 306C7B3 staining for aggregated α-synuclein in the white matter fiber tracts only. **c** Control staining against pSer129-positive α-synuclein aggregates demonstrating a similar staining pattern compared to 306C7B3. Scale bars: 500 mm. **d**, **f**, **h** Enlargement of the gray matter area indicated above (black box on the left, approximate location). **e**, **g**, **i** Enlargement of fiber tract staining in the white matter as indicated above (black box on the right, approximate location). Scale bars enlargements: 50 μm.

### Binding of 306C7B3 to pathological α-synuclein-rich deposits in human α-synucleinopathies

We next assessed the binding of 306C7B3 to pathological α-synuclein-rich deposits using postmortem tissue from patients suffering from MSA. As controls, the Syn-1 antibody known to display aggregation-independent α-synuclein binding, and an anti-pSer129-specific α-synuclein antibody were used. Syn-1, in addition to clearly identifying the pathological glial cytoplasmic inclusions in the white matter tracts of the cerebellum, also markedly stained monomeric α-synuclein in the neuropil of the molecular layer, corresponding to the presynaptic localization of monomeric α-synuclein (Fig. 4a). This prominent staining for the physiological α-synuclein is absent in the immunohistochemical staining's with either 306C7B3 or the pSer129-specific antibody (Fig. 4b, c), demonstrating a strong and aggregate-specific binding of 306C7B3 to human pathological α-synuclein-rich deposits. Strong immunoreactivity of cortical and subcortical Lewy bodies and Lewy neurites in PD and DLB as well as cortical and subcortical neuronal and oligodendroglial inclusions in MSA-P and MSA-C (including intranuclear inclusions) could also be demonstrated in additional affected brain regions of patients (Supplementary Fig. 4 and data not shown). Furthermore, 306C7B3 binding was specific to α-synuclein deposits with no immunoreactivity observed to other amyloid deposits characteristic of neurodegenerative diseases such as TDP-43 inclusions in FTLD-TDP and ALS, FUS inclusions in FTLD-FET, tau pathology in PSP and AD, as well as Abeta in AD (Fig. 5).

Based on the affinity and epitope data, the functional activity in the in vitro aggregation assay, the binding to different α-synuclein pathogenic assemblies, and the specific and sensitive staining of human pathological α-synuclein deposits in brain sections of MSA patients, we conclude that 306C7B3 is a highly aggregate specific

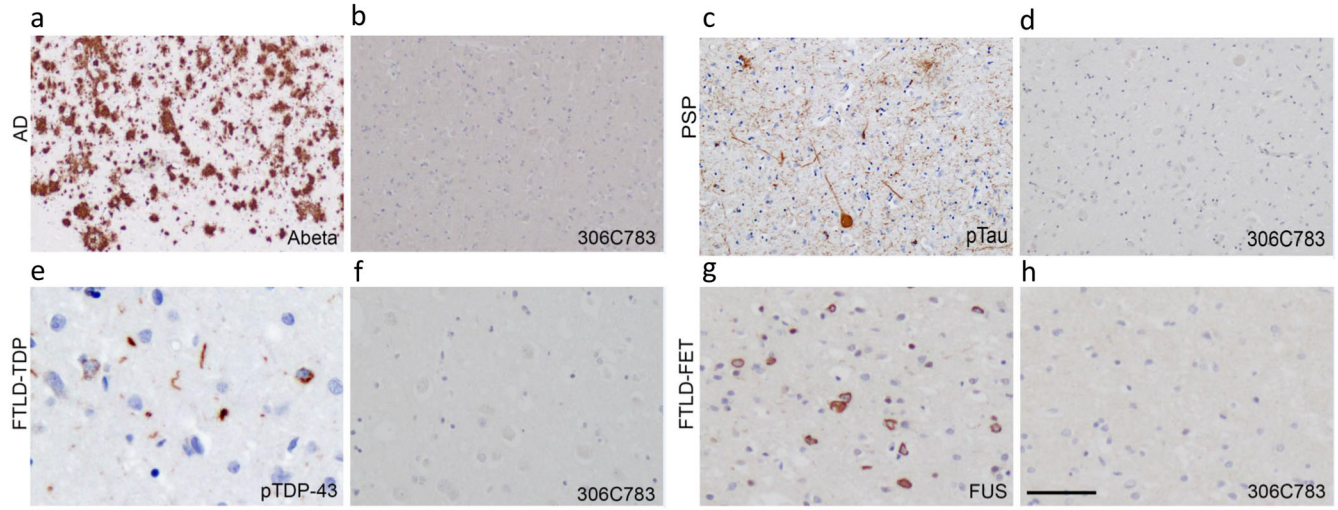


**Fig. 5 306C7B3 does not label other pathological aggregates.** Immunohistochemical analysis of 306C7B3 revealed no labeling of pathological deposits characteristic for other neurodegenerative diseases, including Abeta-positive senile plaques in Alzheimer's disease (AD, **a**, **b**), tau-positive tangles and tufted astrocytes in progressive supranuclear palsy (PSP, **c**, **d**), TDP-43-positive inclusions in frontotemporal lobar degeneration with TDP-43 pathology (FTLD-TDP, **e**, **f**), or FUS-positive inclusions in frontotemporal lobar degeneration with FET pathology (FTLD-FET, **g**, **h**). Immunohistochemistry on formalin fixed paraffin embedded adjacent tissue sections for 306C7B3 (**b**, **d**, **f**, **h**) and Abeta (**a**), pTau (**c**), pTDP-43 (**e**), or FUS (**g**). Scale bar 200 μm (**a**–**d**), 40 μm (**e**–**h**).

anti-α-synuclein antibody devoid of binding toward monomeric α-synuclein, able to block the seeding activity of exogenous α-synuclein fibrils in vitro.

### AAV-mediated antibody expression—selection of AAV serotype

Antibody delivery to the central nervous system is severely hampered by the blood brain barrier, restricting central exposure of full-length antibodies (as measured in the cerebrospinal fluid, CSF) to about 0.2% of the plasma exposure[30]. No major breakdown of the blood brain barrier has been observed in PD or MSA patients[31,32]. To enable significant CSF exposure, we opted for adeno-associated virus (AAV) mediated central transduction with an expression construct for 306C7B3, making use of the scIgG-based, single open-reading frame construct exemplified in Supplementary Fig. 2a, an approach also termed "vectorized immunization"[45]. To establish the route of administration, and to select a suitable AAV serotype, a pilot experiment comparing stereotactic delivery of AAV2 and AAV2HBKO, a variant of AAV2 devoid of heparan sulfate proteoglycan binding[46], into the murine striatum was performed (Fig. 6). Both viral preparations carried an identical transgene coding for GFP under the control of the ubiquitous CMV promoter. Intrastriatal inoculation of the AAV2 based preparation at a total dose of $2.8 \times 10^8$ vector genomes (vg) caused focal, high intensity staining with limited spread of transduction from the site of inoculation. In addition, the center of the transduced striatal area close to the inoculation site contained cellular infiltrates indicative of an inflammatory reaction (Inlets c, d in Fig. 6). In stark contrast, AAV2HBKO transduced striatum (Fig. 6b) showed widespread transduction covering a large portion of the striatum extending into cortical areas in the vicinity of the striatum. No cellular infiltrates were observed in AAV2HBKO-inoculated striata (inlets e, f in Fig. 6). Therefore, the AAV2HBKO serotype was selected for further experiments, allowing for a larger area of transduction with a limited potential to drive inflammatory reactions.

### In vivo α-synucleinopathy model—AAV-mediated expression of scIgG-306C7B3

(Thy-1)-[A30P]-hα-synuclein mice, a transgenic model expressing the familial Parkinson's disease A30P mutation of α-synuclein under the control of the neuronal Thy-1 promoter, develop α-synuclein pathology in a time-dependent manner (ref. [47]; Fig. 7a, b). Previous experiments based on the quantification of pSer-129 α-synuclein load within brain lysates, or extent of central α-synuclein aggregation within the CNS (pSer129 α-synuclein positive staining by immunohistochemistry), exhibited significant variations precluding quantitative analysis (data not shown). We therefore designed a survival study focused on the analysis of the loss of righting reflex as an indicator of severe central α-synucleinopathy[48] to circumvent the variability in onset and aggregate load in this model and to characterize potential effects of 306C7B3 in vivo. Figure 7b shows survival of non-treated control animals. Animals euthanized due to the loss of righting reflex were confirmed to be homozygous for the α-synuclein transgene (Supplementary Fig. 5).

A pilot experiment (Fig. 8) was performed to confirm CNS exposure to scIgG-306C7B3 as well as scIgG-anti-FITC (control, Supplementary Fig. 2b) using a dose of $2.0 \times 10^{10}$ vector genomes of AAV2HBKO per site. Plasma as well as cerebrospinal fluid scIgG-306C7B3 and scIgG-anti-FITC content were analyzed at days 28, 42 and 56 post-inoculation by MSD-based ELISA, and confirmed long-term, chronic exposure. Plasma exposure presumably derived from continuous washout of CSF due to lymphatic drainage was in the range of 50–100 nM (Fig. 8a, b). Even more importantly, strong CSF scIgG-306C7B3 and scIgG-anti-FITC content in the single digit nanomolar range was observed. The ratio between plasma and central CSF scIgG-306C7B3 and scIgG-anti-FITC levels was calculated to be ~12.6 to 1, a value strongly deviating from the ratio achievable after just peripheral administration of antibodies in patients of ~330 to 1[33] or from the naturally observed ratio for antibodies in the healthy situation[30].

Based on this pilot experiment, three doses for AAV2HBKO scIgG-306C7B3 ($2.0 \times 10^9$ vg, $6.3 \times 10^9$ vg and $2.0 \times 10^{10}$ vg per site, bilateral striatal inoculation) were selected for the functional in vivo characterization of scIgG-306C7B3. The control construct—scIgG-anti-FITC—was bilaterally inoculated at the high dose of $2.0 \times 10^{10}$ vg only. In our hands, this animal model never presents with central pSer129-positive α-synuclein pathology if analyzed

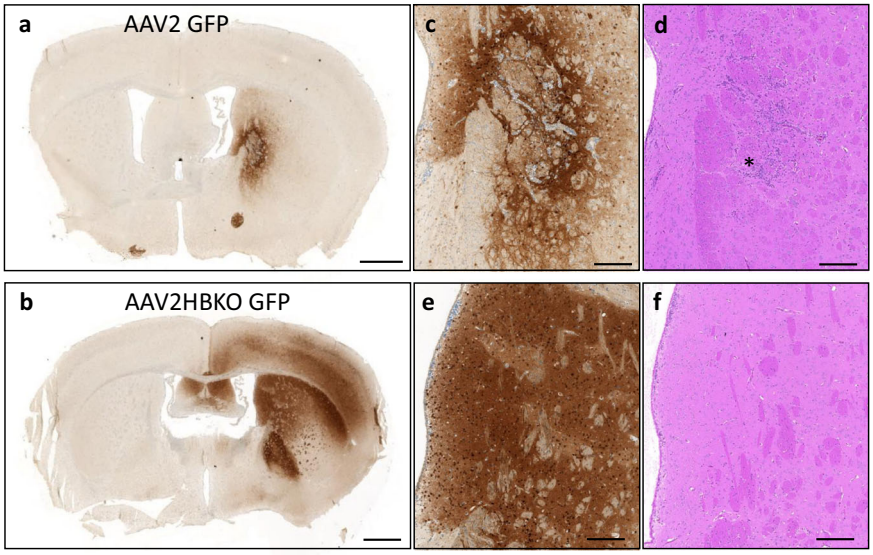


**Fig. 6 Expression of GFP in the murine striatum after AAV inoculation.** One µl of self-complementating (sc) AAV preparations (total of $2.8 \times 10^8$ vector genomes) coding for GFP under the control of the ubiquitous CMV-promoter were stereotactically inoculated into the murine striatum. Immunohistochemical analysis was done 21 days after virus administration. **a** AAV2 based transduction with limited spread of the viral preparation (anti-GFP IHC). **b** Significant spread of the viral transduction observed with AAV2HBKO based viral preparations (anti-GFP IHC). **c**, **e** Enlargement of the transduced striatum (anti-GFP IHC). **d**, **f** H&E staining of adjacent sections in the area of the enlargements (striatum), demonstrating cellular infiltrates in the inoculation area of the AAV2-GFP viral preparation (marked by the asterisk), no such infiltrations were observed in AAV2HBKO treated animals. Scale bars **a**, **b**: 1 mm, enlargements **c**–**f**: 200 µm.

below 14 months of age (Scudamore and Ciossek[48]; and data not shown). Thus, animals at an age of 12 months were selected for initiating treatment via AAV transduction. Only animals with clear symptoms corresponding to α-synucleinopathy within the CNS (loss of righting reflex) were included in the following analysis (see Supplementary Table 1 for details on all animals initially treated and reasons to exclude individual animals).

Figure 7c shows the dose-dependent antibody exposure achieved in this experiment based on the analysis of the final bleed, corresponding to extrapolated CSF exposures of 0.7, 2.5 and 3.9 nM for the low, mid and high doses, respectively (based on CSF exposure data from the pilot experiment, Fig. 8). Efficient, dose-dependent transduction was confirmed for all animals based on vector genomes present in postmortem brain tissue (Fig. 7d).

The functional effect of scIgG-306C7B3 treatment in this model of AAV-mediated antibody expression based on increased survival is shown in Fig. 9. Comparing the non-treated cohort with the scIgG-anti-FITC transduced cohort, no change in survival time could be observed between untreated (Thy-1)-[A30P]-hα-synuclein mice and scIgG-anti-FITC transduced animals ($p = 0.47$, Fig. 9a). This argues for the absence of overt detrimental effects of AAV2HBKO mediated antibody production in the murine striatum. Further comparisons were made toward scIgG-anti-FITC treated animals only to account for potential minor detrimental effects due to viral transduction as well as the consequences of the surgical procedure of stereotactic inoculation into aged mice. Comparison of low and mid doses of AAV2-HBKO coding for scIgG-306C7B3 to the high dose of control AAV2HBKO scIgG-anti-FITC (Fig. 9b) revealed no statistically significant changes in overall survival of treated animals. Interestingly, initial survival seems to be prolonged for about 50 days, although none of the scIgG-306C7B3 treated animals survived longer than the control scIgG-anti-FITC treated animals.

The survival of animals exposed to the high AAV2HBKO scIgG-306C7B3 dose was markedly greater than that of control scIgG-anti-FITC transduced animals (Fig. 9c, $p = 0.03$). Comparison to control animals (not inoculated with viral preparations) also showed a clear increased survival, but just missed statistical significance ($p = 0.09$). Plasma scIgG-306C7B3 levels reached 49.7 nM at the high dose of AAV2-HBKO scIgG-306C7B3 (Fig. 7c).

Finally, all animals were shown to carry strong central α-synuclein pathology as analyzed by pSer129-positive α-synuclein immunohistochemistry (Fig. 10a–e). As expected, no obvious differences in disease severity were observed in this experimental setup, in which all animals were allowed to progress to advanced central pathology (indicated by the loss of righting reflex).

These observations indicate that exposure of the CNS to a neutralizing, anti-aggregate specific α-synuclein antibody could block disease progression in this established animal model for α-synucleinopathies.

## DISCUSSION

As pointed out in the introduction, one widely accepted model accounting for the temporal and spatial progression of pathology in α-synucleinopathies relies on prion-like spread of extracellular α-synuclein aggregates with seeding propensity between neurons. 306C7B3 has been initially developed based on the idea of blocking such prion-like spread of α-synuclein seeds in MSA, DLB or PD patients by passive immunization.

Successful therapeutic application of antibodies or any larger biological entity in synucleinopathies or other neurodegenerative diseases where prion-like spreading occurs must fulfill several important requirements. α-synuclein aggregates with seeding propensity must be spatially accessible to antibodies that prevent their binding to and uptake into non-diseased neuronal or glial cells. The binding moieties of such antibodies should bind efficiently to epitopes present on α-synuclein seeds. It should not bind with high affinity to the monomeric form of the protein (e.g., as observed for PRX002 in a clinical trial[38]). The antibodies should further be devoid of off-target binding. A critical point that must be addressed as well is the achievable exposure level in patients. The central nervous system is known to represent an immune-privileged organ shielded from the peripheral environment by the blood brain barrier that severely limits antibody access to the human brain. This has for example been recently

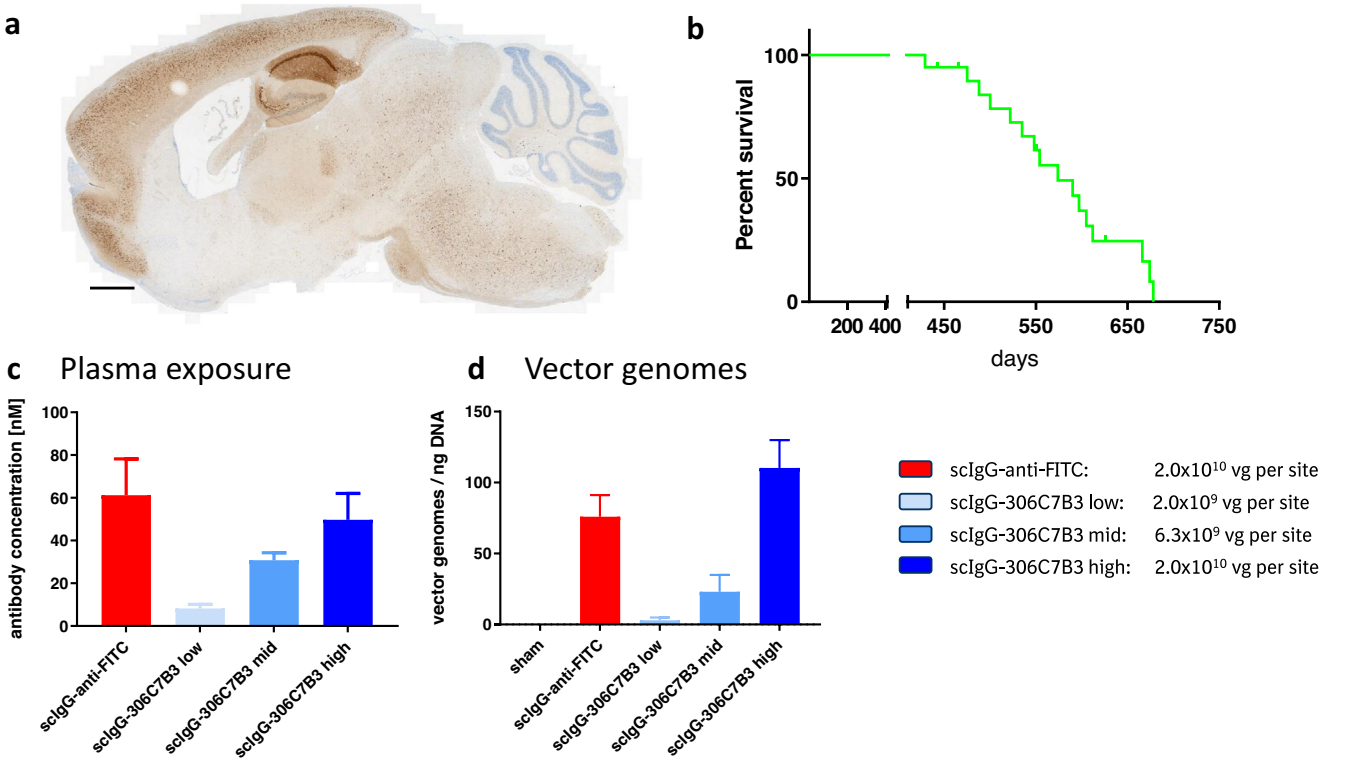


**Fig. 7 In vivo model to assess functional activity of the scIgG-306C7B3. a** Sagital section of the brain of a (Thy-1)-[A30P]-hα-synuclein mouse overexpressing mutant A30P α-synuclein under the control of the neuronal Thy-1 promoter euthanized due to a loss of righting reflex. Shown is a staining for pSer129-positive α-synuclein aggregates. Most aggregates are found in the hindbrain regions and areas of the Medulla oblongata. Scale bar 1 mm. **b** Kaplan–Meier plot of non-treated (Thy-1)-[A30P]-hα-synuclein mice demonstrating age-dependent survival based on loss of righting reflex. **c** Animals received bilateral stereotactic inoculation of each 1 µl of AAV2HBKO preparations carrying transgenes coding for either scIgG-306C7B3 or scIgG-antiFITC control antibody at the indicated viral titers (left). Animals were inoculated at the age of 12 months and analyzed for plasma exposure after loss of righting reflex (mean plus s.e.m.) analyzed with MSD-based ELISAs corresponding to the analyzed samples. No CSF samples had been taken from the actual in vivo study analyzing the functional activity of scIgG-306C7B3 for practical reasons. **d** Post-mortem analysis of brain tissue for transduction efficacy (vg = vector genomes per ng of genomic DNA), demonstrating dose-dependent transduction (mean plus s.e.m.). Sham = non-inoculated controls.

confirmed in the clinical trials for PRX002[33] and BIIB054[34] for PD patients and might explain the recently reported clinical failures of these approaches despite applying high intravenous infusions of the antibodies (refs. [49,50]; potential reasons for failure discussed in detail by ref. [51]). This limited central exposure might also underlie the overall small or missing treatment effects so far observed in similar trials targeting the aggregated, extracellular amyloid-beta (A-beta) deposits in Alzheimer's disease, in addition to other potential reasons like the sometimes observed severe adverse effect (ARIAs, amyloid related imaging abnormalities suggestive of vasogenic edema), late initiation of treatment or inappropriate dose selection[52,53]. The jury is still out regarding the ongoing active immunization approach with UB-312 (currently in clinical trials[54]), inducing a repertoire of C-terminal antibodies against aggregate forms of α-synuclein with some similarities toward 306C7B3[55,56].

We describe the characteristics of a new anti-α-synuclein antibody exhibiting high affinity toward aggregated forms of this protein and poor, if any, binding to monomeric α-synuclein. In surface plasmon binding experiments the antibody displayed a very low off-rate with an overall calculated affinity of around 15 pM toward pre-formed fibrillar α-synuclein. Despite exhibiting recognition toward a relatively large amino acid stretch within the α-synuclein C-terminal end, the PEPperPrint epitope analysis suggests that the epitope most recognized by 306C7B3 spans residues 133–139 (Fig. 2). We therefore conclude that 306C7B3 recognizes a specific conformation that the α-synuclein C-terminal end adopts within its fibrillar form. We further conclude that the conformation 306C7B3 recognizes is not affected by Ser129 phosphorylation (Fig. 1).

306C7B3 binds with high affinity to structurally distinct fibrillar polymorphs and on fibrillar assembly α-synuclein oligomeric species. We conclude from this observation that the α-synuclein C-terminal end adopts the same conformation within all fibrillar species (Fig. 3). More importantly, strong staining of human pathological α-synuclein aggregates in patient samples suffering from MSA or PD/DLB was demonstrated. No binding to pathological protein deposits in other neurodegenerative diseases like Alzheimer's disease, frontotemporal dementia or progressive supranuclear palsy, all known not to carry α-synuclein deposits, was observed. This suggests high specificity of 306C7B3 for pathological α-synuclein aggregates (Figs. 4 and 5).

306C7B3 had been generated by classical immunization with in vitro aggregated, purified human α-synuclein, not carrying post-translational modifications (PTMs). Human α-synuclein is phosphorylated, ubiquitinated, acetylated and nitrated but the only residues that are subject to phosphorylation or nitration are S129, Y133 and Y136 within the α-synuclein C-terminal end (reviewed in ref. [57]), with pSer-129 modification being present in about 90% of the α-synuclein derived from pathological deposits[58]. Human α-synuclein is also subject to truncation at residues 133 and 134. As discussed in a recent review[59], due to several technical limitations the fraction of truncated α-synuclein in postmortem samples can only be roughly estimated and seems to be in the range of

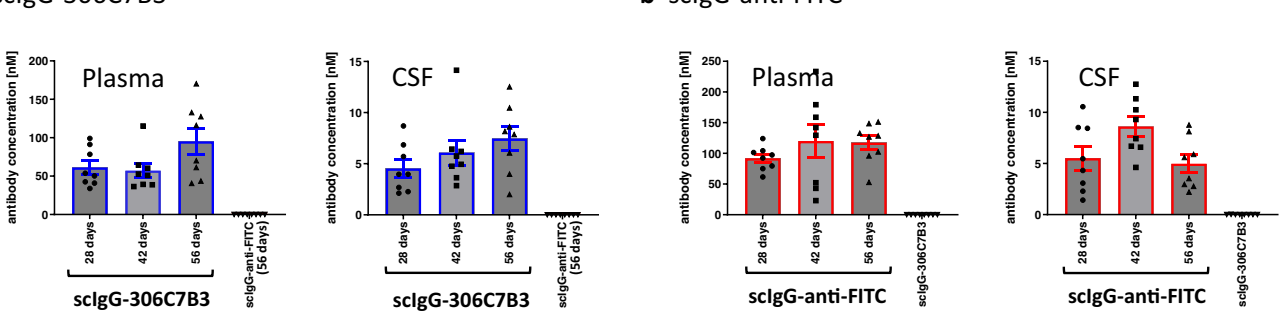


**Fig. 8 Pilot pharmacokinetic study to determine scIgG-306C7B3 and scIgG-anti-FITC exposure.** (Thy-1)-[A30P] hα-synuclein mice were unilaterally inoculated into the striatum at $2.0 \times 10^{10}$ vector genomes with either AAV2HBKO-scIgG-anti-FITC or AAV2HBKO-scIgG-306C7B3. Plasma as well as CSF fluid was analyzed in transduced animals after 28, 42 and 56 days (separate cohorts for each individual time point). **a** Plasma and cerebrospinal fluid (CSF) exposure measuring 306C7B3 with a MSD based ELISA. **b** Plasma and CSF exposure of the control anti-FITC antibody. Analysis as in (**a**). Taking all data together, an approximate ratio of plasma to CSF exposure of 12.6:1 has been calculated for scIgG-306C7B3. Data presented as mean plus s.e.m. ($n = 8$ animals per group).

~15–30% of total deposited α-synuclein with the majority of α-synuclein detected via MS-based analysis corresponding to the full-length protein, with abundancies of 0.23 to 0.26 of 1–122, 1–135, and 1–119 truncated forms compared with full-length 1–140 α-synuclein (set to 1.00[60]). Our immunohistochemical analysis of patient material argue for strong binding of 306C7B3 to pathogenic α-synuclein deposits despite PTMs and partial truncations.

It remains unclear which form of α-synuclein drives pathology, especially regarding the assumed pathological seeds underlying the spatial and temporal disease progression in patients. The fact that 306C7B3 strongly stains pathological deposits in postmortem brain samples argues for its potential to binds such seeds, pointing to the possibility that only a minor fraction of the α-synuclein in these seeds is C-terminally truncated.

As indicated previously, sufficient central exposure with therapeutic antibodies is key for treatment efficacy and this is severely limited due to the blood brain barrier preventing significant transfer of peripheral antibodies into the brain[30]. This has been shown in preclinical animal models of neurodegeneration like e.g., Alzheimer's disease[61], but also seen in recent clinical trials of passive immunization against α-synuclein[33,34]. We have previously performed a passive immunization study with a similar antibody. Here, up to 30 mg/kg of the therapeutic antibody was applied twice per week via intraperitoneal application for 15 weeks into (Thy-1)-[A30P]-hα-synuclein mice. Pathology was induced by prior stereotactic bilateral inoculation of hα-synuclein PFFs into the striatum, based on the observed pathological spread of disease described by ref. [62]. Although high plasma exposure in the single digit-micromolar range was achieved, no significant treatment efficacy could be observed (data not shown). A similar study approach in (Thy-1)-[A30P]-hα-synuclein mice[63], albeit not applying PFF-inoculation mediated pathology induction, also reported no significant effects on fibrillar forms of α-synuclein in insoluble fractions of the brain or spinal cord. Interestingly, the authors reported a trend toward increased survival of treated animals, which they attributed to a reduction in soluble and membrane-associated protofibrils in the spinal cord but not in the brain[63].

We decided to explore AAV-based antibody expression, a gene therapy-based approach driving antibody expression directly within the tissue of interest[64], to address the problem of insufficient permeation of antibodies through an intact blood brain barrier. Such approaches have been tested so far mostly in diseases requiring peripheral exposure[65,66], but have been reported also regarding central transduction mediating antibody exposure within the brain[45,67,68]. At least one trial targeting HIV transmission by intramuscular application also reached clinical stage (Phase I clinical testing[69]), albeit facing problems regarding sufficient transgene expression.

The expression of secreted antibodies within the CNS will not only expose successfully transduced neurons to the therapeutic principle but also allow these antibodies to be present within the intrastitial fluid (ISF) as well as the CSF. The glymphatic pathway, a convective influx from CSF into paravascular spaces mostly driven by aterial pulsatility[70], will distribute these antibodies throughout the whole brain including the spinal cord[71,72], ensuring widespread central distribution even into non-transduced brain areas. CSF is constantly cleared via lymphatic pathways into the peripheral circulation[73,74], explaining the observed plasma exposures in our experiment.

Transduction with AAV2HBKO drove dose-dependent plasma exposure with scIgG-306C7B3 of up to 49.7 nM with a calculated CSF exposure of 3.9 nM, well in line with the experimental approach of central antibody expression combined with clearance into and accumulation in the peripheral blood circulation. Survival was analyzed to circumvent the variability in onset and aggregate load in the (Thy-1)-[A30P]-hα-synuclein model[75], with the loss of the righting reflex of affected animals as criterion closely correlated to disease progression[48,75]. No detrimental effects of neuronal expression of our control scIgG-anti-FITC antibody could be observed, demonstrating the general feasibility of such an approach. Interestingly, the low and mid dose of AAV2HBKO scIgG-306C7B3 showed signs for efficacy without overall increased survival, with efficacy indicated at younger age (Fig. 9b). Statistically significant increased survival was only observed with the high AAV2HBKO dose, correlating with the higher overall plasma and CSF exposure. These data indicate that an initial protective effect of 306C7B3 might be overwhelmed by disease progression at later timepoints. It is important to consider that the (Thy-1)-[A30P]-hα-synuclein model strongly overexpresses mutant [A30P]-hα-synuclein, driving disease induction and progression without additional manipulations like PFF inoculation. Available data suggests that prion-like seeds of α-synuclein are directed to the endolysosomal pathway for degradation and can induce pathological intracellular aggregation only upon endosomal escape[76–78]. Aging is a major risk factor for many neurodegenerative diseases including PD. Evidence exists from preclinical models that the lysosomal activity (measured as macro-autophagy and chaperone-mediated autophagy activity) decreases with aging, although data for the human brain is scarce[79]. We hypothesize that our reported, dose-dependent effects on survival might reflect the ongoing decline of lysosomal activity in the murine brain enabling α-synuclein seed degradation, causing an

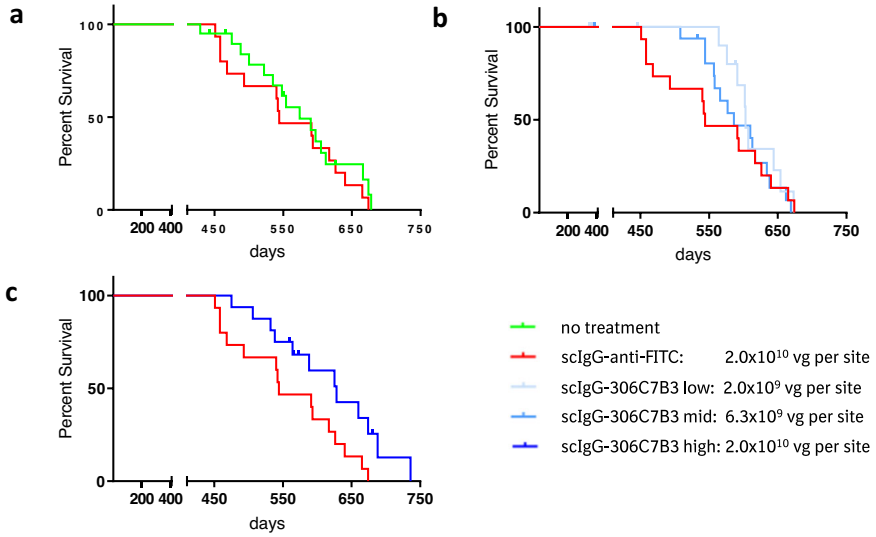


**Fig. 9 In vivo functional activity of scIgG-306C7B3 based on prolonged survival of AAV2-HBKO treated (Thy-1)-[A30P]-hα-synuclein mice.** **a** Comparison of non-treated with control antibody treated (scIgG-anti-FITC) animals. No detrimental effect of the AAV-treatment could be observed ($p = 0.47$). **b** Low and mid doses of AAV2HBKO coding for scIgG-306C7B3 demonstrate delayed initial mortality but no overall increase in survival ($p = 0.99$ and 0.71, respectively). **c** Significant increased survival observed in high dose AAV2HBKO-scIgG-306C7B3 compared to control antibody treated animals ($p = 0.03$; comparison toward non-treated animals $p = 0.09$).

age-dependent increase in prion-like seeds ultimately driving disease progression. Lower exposure with 306C7B3 might be initially sufficient to diminish prion-like disease spreading but this effect might eventually be overwhelmed upon further aging. Although disease progression finally occurs also within the cohort of animals treated with the high dose of AAV2HBKO-scIgG-306C7B3, it appears that the higher CSF exposure with 306C7B3 is sufficient for increased survival. Additional experiments are required to further strengthen this hypothesis.

Several antibodies targeting α-synuclein have been tested in models for α-synucleinopathies to prevent PD-like pathology (see recent reviews by refs. [80–82]), albeit with mixed outcomes. Many approaches went for passive immunization with antibody delivery via intraperitoneal application. Most studies utilized a preventive setting, in which the protective anti-α-synuclein antibody was delivered prior to active disease induction upon PFF inoculation[83–85], potentially compromised by exposure of the inoculated PFFs to the inactivating antibodies during the surgical procedure disrupting the blood brain barrier. In a therapeutic treatment setting using the (Thy-1)-[A30P]-hα-synuclein model[86], significantly weaker effects were reported with pathology reduction mainly analyzed based on reduced pSer129 staining. The effect of the neutralizing antibody was not dose-dependent and potential interference with binding of the utilized pSer129 antibody was not analyzed (epitope of mAb47/ABBV-0805 corresponds to amino acids 121–127 of hα-synuclein, close to the pSer129 site; ref. [86]). MEDI1341, another α-synuclein antibody, has only been analyzed regarding reduction of staining for human α-synuclein without testing for effects on pSer129 α-synuclein staining, indicative of insoluble α-synuclein aggregates. Questions toward the MEDI1341-mediated masking of the utilized Syn-1 IHC staining remain[87]. Yet another approach[88] went for a therapeutic application of Syn9048 in wildtype mice with PFF inoculation-induced pathology, however no significant improvements in behavioral testing and only minor improvements in α-synuclein pathology in some specific brain areas were found, combined with an attenuation of dopamine reductions in the striatum. Recently, efficacy of conformation-specific α-synuclein antibodies was described upon peripheral administration in the Line61 mThy1-α-syn Tg model[89]. The underlying reason for this discrepancy to our previous, unpublished data with passive immunization in the (Thy-1)-[A30P]-hα-synuclein model remains unclear, however the Line61 model displays significantly weaker overall pathology in the brain. The same is true for the reported protective effects of active immunization with UB-312 in the Thy1SNCA/15 mouse model, with improvements in behavior scores and reductions in the levels of α-synuclein oligomer levels 15 weeks after immunization. However, the main protective effects are observed in the colon in this model, potentially hinting toward a main effect on diminishing spreading of pathology from the colon to the CNS[56].

Quite similar approaches to the one described in this publication have been followed recently[90,91] with AAV-mediated expression of fibril-specific α-synuclein binding nanobodies within the CNS. However, these approaches target intracellular α-synuclein by expression of single-chain intrabodies that are not secreted and that exert protective effects only within transduced cells. Such an approach is currently not translatable to clinical use requiring targeting the whole human brain being ~3000 times larger than the murine brain. Recently described approaches use single-chain variable fragment constructs (scFv), with either higher blood brain barrier permeability and a potential for higher cellular uptake[92], or of a bispecific antibody construct targeting α-synuclein as well as the transferrin receptor for increased central uptake[93]. Both approaches suffer from relative short plasma exposures with higher clearance of the proteins from the circulation than observed with more classical antibody immunizations, potentially necessitating shorter treatment intervals in a clinical setting.

The presented work has some limitations. Based on our prior experience regarding variability in the utilized animal model, we limited our analysis on survival of aging transgenic animals naturally developing neuropathology over time. Although we verified that all animals had severe central pSer129 positive α-synuclein aggregations at time of euthanasia, further biochemical and pathophysiological analysis of the degree of neurodegeneration in areas like the substantia nigra, the dorsal motor nucleus of the vagus nerve or the olfactory bulb is missing, not allowing for a more precise analysis of treatment effects on neurodegenerative processes. A follow-up study should look at different timepoints to better pinpoint effects of 306C7B3 treatment on disease progression, something not possible within the context of a survival study with all animals progressing to the final stage of the pathology by

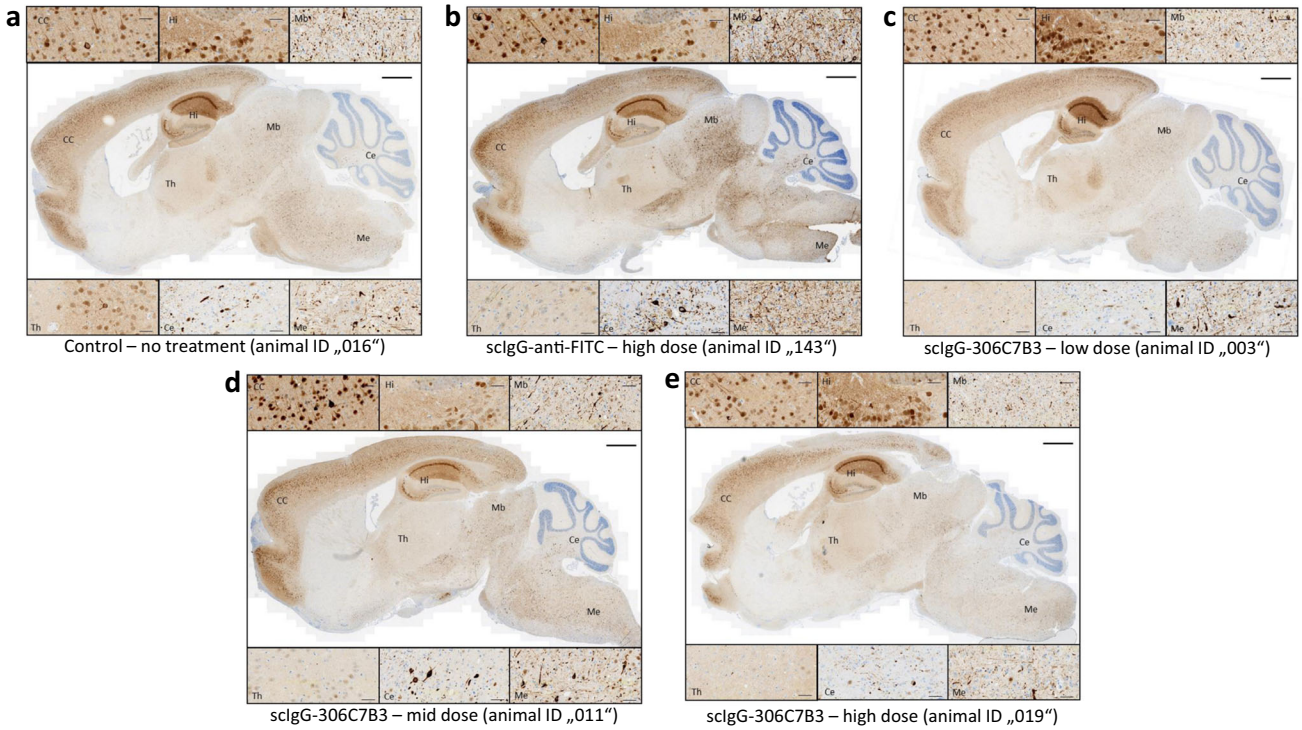


**Fig. 10 IHC analysis of the animals involved in the in vivo study.** Formalin-fixed brain tissue from all animals included in the study were tested via pSer129-α-synuclein immunohistochemistry for strong pathology, corresponding to the symptom of loss of righting reflex at time of euthanasia. Examples of the obtained staining's for representative animals from each cohort are shown (**a**–**e**). See Supplementary Table 1 for details on the individual animals. High magnifications of the indicated areas are shown above and below the full brain images. CC cerebral cortex, Hi hippocampus, Mb midbrain, Th thalamus, Ce cerebellum, Me medulla. Scale bar full brain image: 1 mm, higher magnifications: 50 µm.

study design. The same is true regarding effects on inflammatory reactions due to central pathology. No inflammatory markers were tracked during our experiments due to the fragile nature of aged (Thy-1)-[A30P]-hα-synuclein mice. To avoid treatment-related animal deaths, no such measurements were done. Follow-up studies should incorporate this, including a histological analysis of microglia activation and/or astrocytic gliosis at different time-points post AAV-transduction. Finally, the (Thy-1)-[A30P]-hα-synuclein mouse model is well known to express supraphysiological levels of a human pathogenic variant of α-synuclein, well beyond the expression levels usually observed in patients suffering from α-synucleinopathies. To further substantiate our findings, similar experiments should be performed in other models of α-synucleinopathies like the PFF intrastriatal injection models, allowing for a more precise temporal and spatial control of disease onset.

We are not aware of other descriptions of AAV viral vector mediated expression of a secreted, full-length anti-α-synuclein antibody in a mouse model for α-synucleinopathies resulting in prolonged survival. Based on its specific properties, we believe that this approach of central, AAV-mediated expression of 306C7B3 presents an interesting treatment option for PD or MSA. In addition, application of 306C7B3 for diagnostic purposes deserves further consideration and should be analyzed in more detail in a follow-up study.

## METHODS

### Expression and purification of recombinant monomeric human α-synuclein, and generation of aggregated polymorphs

Expression and purification of monomeric human and mouse α-synuclein used for immunizations and affinity determinations was performed as described[94]. To generate aggregated polymorphs, human wild type α-synuclein was purified as described[95]. Monomeric α-synuclein was aggregated into the fibrillar polymorphs "Fibrils" and "Ribbons" as described previously[40] and into the polymorphs "Fibrils 91" and "Fibrils 65" as described in ref. [42]. "Fibrils 110" that are made of human α-synuclein lacking 30 C-terminal amino-acid residues was generated as described in ref. [43]. The oligomeric forms OGA, ODA and O550 of α-synuclein were generated and purified as described in ref. [44]. All assemblies were assessed by transmission electron microscopy (TEM) after adsorption onto carbon-coated 200 mesh grids and negative staining with 1% uranyl acetate using a Jeol 1400 transmission electron microscope and the images were recorded with a Gatan Orius CCD camera (Gatan, Pleasanton).

### Preparation of fibrillar α-synuclein phosphorylated at Ser129

For generation of pSer129 positive fibrillar α-synuclein preparations, monomeric human α-synuclein (2.5 mg/ml) was in vitro phosphorylated overnight at 30 °C by incubation with purified PLK3 kinase (4.2 µg/ml, #PV3812, Thermo Fisher) in a buffer consisting of 20 mM Hepes pH 7.4, 15 mM MgCl2, 1 mM Mg-ATP, and 2 mM DTT (protocol kindly provided by A. Oueslati and H. Lashuel). Successful phosphorylation was confirmed by mass spectroscopy indicating full pSer129 phosphorylation. Buffer exchange to enable fibril formation was performed using PD 10 spin columns. pSer129-phosphorylated as well as non-phosphorylated fibrils were fragmented in a Covaris S2 Focus-Ultrasonic device (cycle protocol, 6 cycles with varying intensities of up to 10 and durations from 10 to 20 s).

### Hybridoma screening

Hybridoma screening had been performed in collaboration with nanoTools Antikörpertechnik GmbH (Teningen, Germany). For immunization, fibrils of human α-synuclein were further purified to reduce contamination with residual monomeric protein. In brief, preparations were centrifuged at 100,000 × *g* for 1 h to sediment aggregated α-synuclein and the resulting pellet was resuspended three times with PBS followed by additional ultracentrifugations under identical conditions. Final preparations were fragmented in a classical ultrasonic water bath for 8 h, aliquoted and stored at −80 °C. After confirmation of bioactivity (see functional in vitro assay), mice were immunized with fibrils of human α-synuclein and underwent two additional immunizations 5 and 9 weeks after initial priming to boost antibody generation. Obtained hybridoma supernatants were tested in a Luminex bead-based ELISA for binding toward human fibrillar α-synuclein. Positive clones were counter-selected based on binding to monomeric human α-synuclein and confirmed to bind to murine fibrillar α-synuclein.

### Purification of antibodies

Recombinant antibodies (sclgG constructs) were purified after transient transfection of HEK-293 cells with the relevant expression constructs as described in the supplementary materials. Cell culture supernatants of transfected HEK-293 cells cultured in serum-free medium were collected 48 h post-transfection and loaded onto a protein-A based column (AKTApurifier system, Mab Select SuRe 5 ml pre-packed column). After extensive washing with PBS, 1 M NaCl, antibodies were eluted with 30 mM Sodium Acetate, pH 3.6 follow by size exclusion chromatography with 20 mM Na Citrate, 115 mM NaCl, pH 6.0 as running buffer. A similar protocol was used for the purification of native IgG from cultivated hybridoma clones.

### Primary neuron assay

Primary cortical neurons from E16.5 mouse embryos from (Thy-1)-h[A30P]-α-synuclein mice were prepared by papain-mediated cellular dissociation of isolated cortical tissue and cultivated on poly-L-lysine coated 96-well microtiter plates at a seeding density of 5000 cells per well in Neurobasal medium with B27 supplement. Pre-formed fibrillar α-synuclein (100 ng/well) was preincubated with anti-α-synuclein antibodies (1 µg) for 3 h at room temperature and afterwards added to the culture medium. Cells were fixed 21 days post inoculation and stained for pSer129 phosphorylated α-synuclein (Epitomics, #2014-1) and the neuronal marker MAP2 (Encor, #CPCA-MAP2).

### In vitro functional assay analyzing intracellular aggregation of α-synuclein

306C7B3 or other antibody preparations were pre-incubated at the indicated amounts (100 ng to 3 µg) with 50 µg monomeric human α-synuclein pre-filtered through Amicon Ultra-4 centrifugation filter tubes (100 K, 4 ml, #UFC 810024) for 3 h at room temperature to fully saturate monomer-binding antibodies. To each preparation 60 ng of fibrillar α-synuclein was added and further incubated for 30 min at room temperature to allow antibody binding to fibrillar α-synuclein. 1.5 million SH-SY5Y cells stably overexpressing human A53T-mutated α-synuclein[94] were resuspended in electroporation buffer R (NEON electroporation system, Thermo Fisher) and added to the antibody-fibril preparation (final volume 100 µl). Cells were pulsed once at a voltage of 1200 V for 30 milliseconds. The electroporated cells were immediately diluted into 8 ml differentiation media for SH-SY5Y cells[96] and seeded in collagen-IV coated flat-bottom 384 well microtiter plates amenable for high content analysis (Greiner) at a concentration of 10,000 cells per well in 80 µl total volume. Cells were incubated at 37 °C for 2 days in a standard cell culture incubator. Percentage of cells carrying intracellular α-synuclein aggregates was analyzed after fixation in an InCell High Content Analyzer via immunofluorescence staining against pSer129 phosphorylated α-synuclein (anti-pSer129 antibody, Epitomics, #2014-1).

### Filter trap assay against different aggregate assemblies of human α-synuclein

Monomeric human α-synuclein and different fibrillar polymorphs (fibrils, ribbons, fibrils 65, fibrils 91, fibrils 110) and oligomeric species (on fibrillar assembly pathway α-synuclein oligomers O550, dopamine-stabilized ODA and glutaraldehyde-stabilized OGA oligomers) in the range of 20 pg to 200 ng were spotted on nitrocellulose filters (Ref Protran 0.45 µm NC) using a slot blot filtration apparatus (GE Healthcare). The filters were blocked with skimmed milk and incubated with 306C7B3 IgG at 0.1 µg/ml. After extensive washing, binding of 306C7B3 was revealed using a goat anti-mouse secondary antibody with Super Signal ECL (Pierce #34096). The blots were imaged on a BioRad imager (Chemidoc MP imaging system/BioRad imagelab software).

### Affinity measurements

Antibody affinities were measured by surface plasmon resonance on a Biacore T2000 instrument. For monomeric α-synuclein, anti-murine IgG was immobilized on a CM5 chip. Test antibodies were captured using a 10 µg/ml antibody solution. Binding of monomeric α-synuclein was then analyzed in single-cycle kinetics with 5 concentrations ranging from 1.2 to 100 nM. Fibrillar α-synuclein prepared as described above was further purified by size exclusion chromatography (Superdex 75 10/300 GL column), and purity was confirmed by analytical HPLC (>95%). Fibrils were immobilized on CM5 chips by amine coupling at 20 µg/ml in 10 mM Na-acetate buffer, pH 4.5. Binding of test antibodies was determined in single-cycle kinetics with 5 antibody concentrations ranging from 0.12 to 10 µg/ml. KD values were calculated using a 1:1 binding model adjusted for drift.

### Epitope determination

The identification of the epitope of selected antibodies was performed at PEPperPRINT GmbH (Heidelberg, Germany) utilizing the PEPperMAP epitope mapping technology. In brief, the full sequence of human α-synuclein was elongated at the C- and N-terminus with neutral GSGSGSG linkers and translated into an array of 15 amino acid peptides with a peptide overlap of 14 amino acids. The resulting peptide microarray containing 140 different peptides was printed in duplicate and framed by Flag (DYKDDDDKGG) and HA (YPYDVPDYAG) control peptides. Peptide microarrays were incubated with the antibody in question, followed by washing steps and staining with a secondary goat anti-mouse antibody conjugated with fluorophore dyes. After analysis for signal intensity, an intensity map based on average median foreground intensities was generated and peptides contributing to antibody binding calculated.

### Human postmortem tissue

Sections from paraffin-embedded formalin-fixed human brain tissue samples were obtained from the brain banks affiliated with the University of Tübingen and the DZNE. Written consent for autopsy was obtained from probands or their legal representative in accordance with the approval of the Ethics Committee of the University of Tübingen and the University Hospital Tübingen (386/2017B01). The cohort of α-synucleinopathy cases consisted of six cases with Lewy body diseases (PD, DLB) and three cases with MSA. Control cases for immunohistochemistry included frontotemporal lobar degeneration with TDP-43 pathology (FTLD-TDP; $n = 4$), FTLD with FET pathology (FTLD-FET; $n = 1$), sporadic

amyotrophic lateral sclerosis with TDP-43 pathology (ALS; $n = 2$), progressive supranuclear palsy (PSP; $n = 2$), Alzheimer's disease (AD; $n = 2$), and neurologically healthy controls ($n = 2$).

### Immunohistochemistry

Immunohistochemistry on human postmortem tissues was performed on 3 µm thick sections of formalin fixed, paraffin-embedded (FFPE) tissues from neuroanatomical regions with robust pathology in the respective diseases using the Ventana BenchMark XT automated staining system with the iVIEW DAB detection kit (Ventana). 306C7B3 was used at 1:10,000 dilution with heat pretreatment (boiling for 32 min in CC1 buffer, Ventana). Other antibodies included anti-pS409/410-TDP-43, clone 1D3 (1:500, ref. [97]), anti-ptau, clone AT8 (Thermo Fisher, 1:500), anti-α-synuclein, clone 4D6 (Origene, 1:1000), anti-beta-Amyloid, clone 4G8 (Covance, 1:6000) and anti-FUS (Bethyl Laboratories, 1:400).

In addition, manual staining was done on selected human case and mouse tissue. The tissue sections were deparaffinized in a standard series of xylol and alcohol. Pretreatments varied depending on the individual antibodies employed. For GFP (rabbit polyclonal anti-GFP, Abcam, ab290), sections were incubated for 10 min in enzyme buffer (Bond Enzyme Pretreatment Kit, Leica Biosystems) at 37 °C to assist epitope retrieval. 306C7B3 stainings were done with enzyme pretreatment (Bond Enzyme Pretreatment Kit, Leica Biosystems) at 37 °C for 5 min. Syn-1 stainings (clone 42, BD Biosciences) were done at a dilution of 1:1000. For pSer129 α-synuclein staining (EP1536Y rabbit anti-α-synuclein pSer129 antibody, Epitomics, diluted 1:1000), no pretreatment was required. Color development was performed with classical DAB (3,3'-diaminobenzidine) staining (Bond Polymer Refine Detection Kit, Leica Biosystems.

### AAV production and quantification

Expression plasmids for AAV production were generated by gene synthesis (GeneArt, Thermo Fisher) and subcloned into the pAAV plasmid (AAV Helper-Free System, Agilent). A plasmid map for the sclgG-306C7B3 expression construct is shown in the Supplementary Materials. Viral stocks were generated as described[98] using polyethylenglycol precipitation and iodixanol gradient centrifugation of HEK293 cell lysates. AAVs were dissolved in AAV formulation buffer (PBS, 1 mM MgCl2, 2.5 mM KCl, 10% glycerol, 0.001% Pluronic F-68, pH 7.4) and stored at −80 °C after being sterile-filtered. Titer determination with quantitative PCR was done on extracted viral DNA according to ref. [98] with PCR primers directed against the promoter region of the expression constructs.

### In vivo experiments in (Thy-1)-h[A30P]-α-synuclein mice

All animal experiments were conducted in an AAALAC-accredited facility (Association for Assessment and Accreditation of Laboratory Animal Care International) in accordance with the EU Directive 2010/63/EU for animal experiments. Ethical approval and license for the animal experiments were granted by the responsible local government authority (Fachreferat Tierschutz, Regierungspräsidium Tübingen, Baden-Württemberg, Germany). Mice were given food and water ad libitum, while room temperature and humidity were maintained at 22 °C ± 2 °C and 55% ± 10%, respectively.

For the described experiments homozygous (Thy-1)-h[A30P]-α-synuclein mice (refs. [47,99]; kindly donated by Philipp Kahle) extensively backcrossed (>10 generations) into C57Bl6/J background were used. Phenotype development in this transgenic model is dose dependent with earlier onset of pathology in homozygous compared to heterozygous animals. To ensure homozygosity of the transgene, genotyping was performed on tail biopsies taken from animals after weaning. Genomic tail DNA was purified using QiaAmp DNA Mini Kits and a Qiacube robot (Qiagen), according to the instructions of the manufacturer. Briefly, tail snips were digested overnight at 56 °C with shaking in tissue-lysis buffer containing proteinase K, followed by purification with the provided spin columns. Initially, genotyping was performed with quantitative PCR able to distinguish hemizygous from homozygous animals as described[48]. Later genotyping was done with classical PCR based on primers spanning the integration site of the transgene, resulting in amplified fragments of 287 bp for the transgene allele and 340 bp for the wildtype allele[100].

### Stereotactic injection into the striatum of (Thy-1)-h[A30P]-α-synuclein mice

AAVHBKO viral preparations expressing either sclgG-306C7B3 or a control antibody without a known target in mice (anti-FITC sclgG) were stereotactically injected (1 µl per injection, total titers as described in the figures) bilaterally into the striatum of (Thy-1)-h[A30P]-α-synuclein male and female mice at an age of 12 months ($n = 16$ per group). All surgical procedures were performed using aseptic techniques. Briefly, medetomidin, midazolam, fentanyl (0.5/5/0.05 mg per kg intraperitoneally) was used for anesthesia. After onset of anesthesia, the head was shaved, area disinfected, local anesthetic lidocaine applied, and the animal transferred to a stereotactic head frame. Body temperature was controlled, and animals were kept on a heat pad. A midline anterior posterior incision of the scalp was used to access the skull and lambda and bregma were used for anterior-posterior (+0.1/+0.1 cm), dorsal-ventral (−0.37/−0.36 cm) and medial-lateral (+0.2/−0.2 cm) orientation for bilateral application. Coordinates were internally validated to allow for mid-striatal viral delivery, albeit slightly deviating from the recommend coordinates usually applied for striatal PFF inoculation (see ref. [101] for details). Burr holes were drilled in the appropriate locations and 1 µl of fluid with 200 nl/min was injected into the striatum using a microliter syringe (Hamilton, Reno, Nevada). Injection needle was kept in place for 5 min before careful retraction from the injection side. After cleaning of the skull and stitching of the scalp, Atipamizol, Flumazenil, Naloxon (2.5/0.5/1.2 mg per kg subcutaneous) were given to antagonize anesthesia. For post operative care meloxicam (1 mg per kg subcutaneous) was used.

Animals were constantly monitored for disease progression as indicated by the loss of righting reflex[48], triggering euthanasia of the affected animals. Brain tissue as well as a final blood sample for exposure measurements were prepared and further analyzed as described.

### Vector genome quantification

Vector genomes present in each treated animal was quantified after preparation of genomic DNA from one brain hemisphere with the AllPrep96 DNA/RNA Kit (Qiagen). qPCR with primers and a probe directed against the hSyn promoter sequence (forward 5'-ATGAGTGCAAGTGGGTTTTAGGA-3', reverse 5'-CCCTCCCCCTCTCTG ATAGG-3', probe 5'-CGACCCCGACCCACTGGACAAG-3') was performed to confirm efficient and dose-dependent transduction.

### CSF sampling

CSF was collected from the cisterna magna. Therefore, animals were fixated and anesthetized as described for stereotactic injections. Briefly, after application of local anesthetics the head of the animal was bend and the skin at the neck of animal opened with an incision on the base of the skull. Tissue was bluntly removed to access cisterna magna via occipital membrane. A microliter syringe (Hamilton, Reno, Nevada) was guided via the stereotaxic frame and a micropump (Hamilton, Reno, Nevada) was used to withdraw fluid at a speed of 1000 nl/min.

### ELISAs to measure 306C7B3 and anti-FITC antibodies

An MSD-based ELISA was established to measure exposure of 306C7B3 in plasma and CSF mouse samples, similar to the description provided in ref. [102]. Briefly, MSD standard plates (MSD #L15XA-1) were coated overnight with 100 ng fibrillar human α-synuclein (diluted to 30 µl per well with PBS) at 4 °C overnight. After washing to remove unbound fibrillar α-synuclein, plasma or CSF probes were incubated in 25 µl for 1 h at room temperature (diluted with PBS containing 5% Amersham ECL Blocking Agent, GE Healthcare RNP2125), followed by additional washing steps and incubation with an anti-mouse secondary antibody conjugated with the MSD Sulfo-tag for detection. A similar protocol was established to measure the control anti-FITC antibody utilizing FITC-conjugated BSA (A23015, Molecular Probes) to capture the antibody[102].

### Statistical analysis

The in vivo data were statistically analyzed based on a Cox regression model with time to death as dependent variable and treatment, gender, and cause of death as independent factors. No adjustments of the significance level for multiple testing were made, all *p* values have to be interpreted as part of the descriptive and exploratory analysis. The statistical evaluation was prepared using the software SAS Version 9.4 (SAS Institute Inc., Cary, North Carolina, USA).

## DATA AVAILABILITY

Data supporting the findings of this study (high resolution IHC figures, raw data) are available from the corresponding author upon request. Sequence files specifying the amino acid sequence of 306C7B3, and the anti-FITC control antibody are available from the corresponding author.

Received: 2 December 2022; Accepted: 5 June 2023;
Published online: 15 June 2023

## REFERENCES

1. Shahmoradian, S. H. et al. Lewy pathology in Parkinson's disease consists of crowded organelles and lipid membranes. *Nat. Neurosci.* **22**, 1099–1109 (2019).
2. Oliveira, L. M. A. et al. Alpha-synuclein research: defining strategic moves in the battle against Parkinson's disease. *NPJ Parkinsons Dis.* **7**, 65 (2021).
3. Spillantini, M. G. et al. Alpha-synuclein in Lewy bodies. *Nature* **388**, 341–346 (1997).
4. Goedert, M., Spillantini, M. G., Del Tredici, K. & Braak, H. 100 years of Lewy pathology. *Nat. Rev. Neurol.* **9**, 13–24 (2013).
5. Schneider, S. A. & Alcalay, R. N. Neuropathology of genetic synucleinopathies with parkinsonism: review of the literature. *Mov. Disord.* **32**, 1504–1523 (2017).
6. Polymeropoulos, M. H. et al. Mutation in the alpha-synuclein gene identified in families with Parkinson's disease. *Science* **276**, 2045–2047 (1997).
7. Singleton, A. B. et al. Alpha-synuclein locus triplication causes Parkinson's disease. *Science* **302**, 841 (2003).
8. Chartier-Harlin, M. C. et al. Alpha-synuclein locus duplication as a cause of familial Parkinson's disease. *Lancet* **364**, 1167–1169 (2004).
9. Simon-Sanchez, J. et al. Genome-wide association study reveals genetic risk underlying Parkinson's disease. *Nat. Genet.* **41**, 1308–1312 (2009).
10. Brockmann, K. et al. SNCA: major genetic modifier of age at onset of Parkinson's disease. *Mov. Disord.* **28**, 1217–1221 (2013).
11. Iwai, A. et al. The precursor protein of non-A beta component of Alzheimer's disease amyloid is a presynaptic protein of the central nervous system. *Neuron* **14**, 467–475 (1995).
12. Vargas, K. J. et al. Synucleins regulate the kinetics of synaptic vesicle endocytosis. *J. Neurosci.* **34**, 9364–9376 (2014).
13. Huang, M. et al. α-Synuclein: a multifunctional player in exocytosis, endocytosis, and vesicle recycling. *Front. Neurosci.* **13**, 28 (2019).
14. Abeliovich, A. et al. Mice lacking alpha-synuclein display functional deficits in the nigrostriatal dopamine system. *Neuron* **25**, 239–252 (2000).
15. Greten-Harrison, B. et al. αβγ-Synuclein triple knockout mice reveal age-dependent neuronal dysfunction. *PNAS USA* **107**, 19573–19578 (2010).
16. Burre, J. et al. Alpha-synuclein promotes SNARE-complex assembly in vivo and in vitro. *Science* **329**, 1663–1667 (2010).
17. Sulzer, D. & Edwards, R. H. The physiological role of α-synuclein and its relationship to Parkinson's disease. *J. Neurochem.* **150**, 475–486 (2019).
18. Luk, K. C. et al. Pathological α-synuclein transmission initiates Parkinson-like neurodegeneration in nontransgenic mice. *Science* **338**, 949–953 (2012).
19. Sacino, A. N. et al. Intramuscular injection of α-synuclein induces CNS α-synuclein pathology and a rapid-onset motor phenotype in transgenic mice. *PNAS USA* **111**, 10732–10737 (2014).
20. Peelaerts, W. et al. α-Synuclein strains cause distinct synucleinopathies after local and systemic administration. *Nature* **522**, 340–344 (2015).
21. Sorrentino, Z. A. et al. Intrastriatal injection of α-synuclein can lead to widespread synucleinopathy independent of neuroanatomic connectivity. *Mol. Neurodegener.* **12**, 40 (2017).
22. Braak, H. et al. Staging of brain pathology related to sporadic Parkinson's Disease. *Neurobiol. Aging* **24**, 197–211 (2003).
23. Li, J. Y. et al. Lewy bodies in grafted neurons in subjects with Parkinson's disease suggest host-to-graft disease propagation. *Nat. Med.* **14**, 501–503 (2008).
24. Kordower, J. H., Chu, Y., Hauser, R. A., Freeman, T. B. & Olanow, C. W. Lewy body-like pathology in long-term embryonic nigral transplants in Parkinson's disease. *Nat. Med.* **14**, 504–506 (2008).
25. Brundin, P. & Melki, R. Prying into the prion hypothesis for Parkinson's disease. *J. Neurosci.* **37**, 9808–9818 (2017).
26. Manne, S. et al. Ultrasensitive detection of aggregated α-synuclein in glial cells, human cerebrospinal fluid, and brain tissue using the RT-QuIC assay: new high-throughput neuroimmune biomarker assay for Parkinsonian disorders. *J. Neuroimmune Pharmacol.* **14**, 423–435 (2019).
27. Fairfoul, G. et al. Alpha-synuclein RT-QuIC in the CSF of patients with alpha-synucleinopathies. *Ann. Clin. Transl. Neurol.* **28**, 812–818 (2016).
28. Shahnawaz, M. et al. Development of a biochemical diagnosis of Parkinson disease by detection of α-synuclein misfolded aggregates in cerebrospinal fluid. *JAMA Neurol.* **74**, 163–172 (2017).
29. Brundin, P., Dave, K. D. & Kordower, J. H. Therapeutic approaches to target alpha-synuclein. *Exp. Neurol.* **298**, 225–235 (2017).
30. Reiber, H. Dynamics of brain-derived proteins in cerebrospinal fluid. *Clin. Chim. Acta* **310**, 173–186 (2001).
31. Jesse, S. et al. Summary of cerebrospinal fluid routine parameters in neurodegenerative diseases. *J. Neurol.* **258**, 1034–1041 (2011).
32. Song, S. K. et al. Blood-brain barrier impairment is functionally correlated with clinical severity in patients of multiple system atrophy. *Neurobiol. Aging* **32**, 2183–2189 (2011).
33. Jankovic, J. et al. Safety and tolerability of multiple ascending doses of PRX002/RG7935, an anti-α-synuclein monoclonal antibody, in patients with Parkinson disease: a randomized clinical trial. *JAMA Neurol.* **75**, 1206–1214 (2018).
34. Brys, M. et al. Randomized phase I clinical trial of anti-α-synuclein antibody BIIB054. *Mov. Disord.* **34**, 1154–1163 (2019).
35. Poewe, W. et al. Safety and tolerability of active immunotherapy targeting α-synuclein with PD03A in patients with early Parkinson's disease: a randomized, placebo-controlled, phase 1 study. *J. Parkinsons Dis.* **11**, 1079–1089 (2021).
36. Barbour, R. et al. Red blood cells are the major source of alpha-synuclein in blood. *Neurdegener. Dis.* **5**, 55–59 (2008).
37. Koehler, N. K. U. et al. Alpha-synuclein levels in blood plasma decline with healthy aging. *PLoS ONE* **10**, e0123444 (2015).
38. Schenk, D. B. et al. First-in-human assessment of PRX002, an anti-α-synuclein monoclonal antibody, in healthy volunteers. *Mov. Disord.* **32**, 211–218 (2017).
39. Polinski, N. K. et al. Best practices for generating and using alpha-synuclein pre-formed fibrils to model Parkinson's disease in rodents. *J. Parkinsons Dis.* **8**, 303–322 (2018).
40. Bousset, L. et al. Structural and functional characterization of two alpha-synuclein strains. *Nat. Commun.* **4**, 2575 (2013).
41. Masliah, E. et al. Effects of α-synuclein immunization in a mouse model of Parkinson's disease. *Neuron* **46**, 857–868 (2005).
42. Makky, A., Bousset, L., Polesel-Maris, J. & Melki, R. Nanomechanical properties of distinct fibrillar polymorphs of the protein α-synuclein. *Sci. Rep.* **30**, 37970 (2016).
43. Shrivastava, A. N. et al. Differential membrane binding and seeding of distinct α-synuclein fibrillar polymorphs. *Biophys. J.* **118**, 1301–1320 (2020).
44. Pieri, L., Madiona, K. & Melki, R. Structural and functional properties of prefibrillar α-synuclein oligomers. *Sci. Rep.* **14**, 24526 (2016).
45. Liu, W. et al. Vectorized intracerebral immunization with the anti-tau monoclonal antibody PHF1 markedly reduces tau pathology in mutant tau transgenic mice. *J. NeuroSci.* **36**, 12425–12435 (2016).
46. Naidoo, J. et al. Extensive transduction and enhanced spread of a modified AAV2 capsid in the non-human primate CNS. *Mol. Ther.* **26**, 2418–2430 (2018).

47. Neumann, M. et al. Misfolded proteinase K-resistant hyperphosphorylated alpha-synuclein in aged transgenic mice with locomotor deterioration and in human alpha-synucleinopathies. *J. Clin. Invest.* **110**, 1429–1439 (2002).
48. Scudamore, O. & Ciossek, T. Increased oxidative stress exacerbates α-synuclein aggregation in vivo. *J. Neuropathol. Exp. Neurol.* **77**, 443–453 (2018).
49. Lang, A. E. et al. Trial of cinpanemab in early Parkinson's disease. *N. Engl. J. Med.* **387**, 408–420 (2022).
50. Pagano, G. et al. Trial of prasinezumab in early-stage Parkinson's disease. *N. Engl. J. Med.* **387**, 421–432 (2022).
51. Jensen, P. H., Schlossmacher, M. G. & Stefanis, L. Who ever said it would be easy? Reflecting on two clinical trials targeting a-synuclein. *Mov. Disord.* **38**, 378–384 (2023).
52. Asher, S. & Priefer, R. Alzheimer's disease failed clinical trials. *Life Sci.* **306**, 120861 (2022).
53. Nimmo, J. T. et al. Amyloid-β and α-synuclein immunotherapy: from experimental studies to clinical trials. *Front. Neurosci.* **15**, 733857 (2021).
54. Yu, H. J. et al. A randomized first-in-human study with UB-312, a UBITh α-synuclein peptide vaccine. *Mov. Disord.* **37**, 1416–1424 (2022).
55. Nimmo, J. T. et al. Novel antibodies detect additional a-synuclein pathology in synucleinopathies: potential development for immunotherapy. *Alzheimers Res. Ther.* **12**, 159 (2020).
56. Nimmo, J. T. et al. Immunisation with UB-312 in the Thy1SNCA mouse prevents motor performance deficits and oligomeric α-synuclein accumulation in the brain and gut. *Acta Neuropathol.* **143**, 55–73 (2022).
57. Schmid, A. W., Fauvet, B., Moniatte, M. & Lashuel, H. A. Alpha-synuclein post-translational modifications as potential biomarkers for Parkinson disease and other synucleinopathies. *Mol. Cell. Proteom.* **12**, 3543–3558 (2013).
58. Anderson, J. P. et al. Phosphorylation of Ser-129 is the dominant pathological modification of alpha-synuclein in familial and sporadic Lewy body disease. *J. Biol. Chem.* **281**, 29739–29752 (2006).
59. Sorrentino, Z. A. & Giasson, B. I. The emerging role of α-synuclein truncation in aggregation and disease. *J. Biol. Chem.* **30**, 10224–10244 (2020).
60. Kellie, J. F. et al. Quantitative measurement of intact alpha-synuclein proteoforms from post-mortem control and Parkinson's disease brain tissue by intact protein mass spectrometry. *Sci. Rep.* **4**, 5797 (2014).
61. Bien-Ly, N. et al. Lack of widespread BBB disruption in Alzheimer's disease models: focus on therapeutic antibodies. *Neuron* **88**, 289–297 (2015).
62. Luk, K. C. et al. Intracerebral inoculation of pathological α-synuclein initiates a rapidly progressive neurodegenerative α-synucleinopathy in mice. *J. Exp. Med.* **209**, 975–986 (2012).
63. Lindström, V. et al. Immunotherapy targeting α-synuclein protofibrils reduced pathology in (Thy1)-h[A30P] α-synuclein mice. *Neurobiol. Dis.* **69**, 134–143 (2014).
64. Fuchs, S. P., Martinez-Navio, J. M., Gao, G. & Desrosiers, R. C. Recombinant AAV vectors for enhanced expression of authentic IgG. *PLoS ONE* **11**, e0158009 (2016).
65. Robert, M. A., Gilbert, R. & Gailett, B. Antibody delivery mediated by recombinant adeno-associated virus for the treatment of various chronic and infectious diseases. *Curr. Gene Ther.* **16**, 363–374 (2016).
66. Balazs, A. B. Antibody-based protection against HIV infection by vectored immunoprophylaxis. *Nature* **481**, 81–84 (2012).
67. Ising, C. et al. AAV-mediated expression of anti-tau scFvs decreases tau accumulation in a mouse model of tauopathy. *J. Exp. Med.* **214**, 1227–1238 (2017).
68. Fukuchi, K. et al. Anti-Abeta single-chain antibody delivery via adeno-associated virus for treatment of Alzheimer's disease. *Neurobiol. Dis.* **23**, 502–511 (2006).
69. Priddy, F. H. et al. Adeno-associated virus vectored immunoprophylaxis to prevent HIV in healthy adults: a phase 1 randomised controlled trial. *Lancet HIV* **6**, e230–e239 (2021).
70. Nedergaard, M. Garbage truck of the brain. *Science* **340**, 1529–1530 (2013).
71. Iliff, J. J. et al. A paravascular pathway facilitates CSF flow through the brain parenchyma and the clearance of interstitial solutes, including amyloid β. *Sci. Transl. Med.* **15**, 147 (2012).
72. Iliff, J. J. et al. Brain-wide pathway for waste clearance captured by contrast-enhanced MRI. *J. Clin. Invest.* **123**, 1299–1309 (2013).
73. Sakka, L., Coll, G. & Chazal, J. Anatomy and physiology of cerebrospinal fluid. *Eur. Ann. Otorhinolaryngol. Head. Neck Dis.* **128**, 309–316 (2011).
74. Louveau, A. et al. Structural and functional features of central nervous system lymphatic vessels. *Nature* **523**, 337–341 (2015).
75. Freichel, C. et al. Age-dependent cognitive decline and amygdala pathology in alpha-synuclein transgenic mice. *Neurobiol. Aging* **28**, 1421–1435 (2007).
76. Karpowicz, R. J. Jr. et al. Selective imaging of internalized proteopathic α-synuclein seeds in primary neurons reveals mechanistic insight into transmission of synucleinopathies. *J. Biol. Chem.* **292**, 13482–13497 (2017).
77. Sacino, A. N. et al. Proteolysis of α-synuclein fibrils in the lysosomal pathway limits induction of inclusion pathology. *J. Neurochem.* **140**, 662–678 (2017).
78. Flavin, W. P. et al. Endocytic vesicle rupture is a conserved mechanism of cellular invasion by amyloid proteins. *Acta Neuropathol.* **134**, 629–653 (2017).
79. Loeffler, D. A. Influence of normal aging on brain autophagy: a complex scenario. *Front. Aging Neurosci.* **11**, 49 (2019).
80. Folke, J., Ferreira, N., Brudek, T., Borghammer, P. & Van Den Berge, N. Passive immunization in alpha-synuclein preclinical animal models. *Biomolecules* **12**, 168 (2022).
81. Vijayakumar, D. & Jankovic, J. Slowing Parkinson's disease progression with vaccination and other immunotherapies. *CNS Drugs* **36**, 327–343 (2022).
82. Castonguay, A. M., Gravel, C. & Lévesque, M. Treating Parkinson's disease with antibodies: previous studies and future directions. *J. Parkinsons Dis.* **11**, 71–92 (2021).
83. Weihofen, A. et al. Development of an aggregate-selective, human-derived α-synuclein antibody BIIB054 that ameliorates disease phenotypes in Parkinson's disease models. *Neurobiol. Dis.* **124**, 276–288 (2019).
84. Li, Y. et al. Novel naturally occuring autoantibodies attenuate a-synuclein pathology in a mouse model of Parkinson's disease. *Neuropathol. Appl. Neurobiol.* **49**, e12860 (2023).
85. Brendza, R. et al. Anti-α-synuclein c-terminal antibodies block PFF uptake and accumulation of phosphor-synuclein in preclinical models of Parkinson's disease. *Neurobiol. Dis.* **177**, 105969 (2023).
86. Nordström, E. et al. ABBV-0805, a novel antibody selective for soluble aggregated α-synuclein, prolongs lifespan and prevents buildup of α-synuclein pathology in mouse models of Parkinson's disease. *Neurobiol. Dis.* **161**, 105543 (2021).
87. Schofield, D. J. et al. Preclinical development of a high affinity α-synuclein antibody, MEDI1341, that can enter the brain, sequester extracellular α-synuclein and attenuate α-synuclein spreading in vivo. *Neurobiol. Dis.* **132**, 104582 (2019).
88. Henderson, M. X. et al. Characterization of novel conformation-selective α-synuclein antibodies as potential immunotherapeutic agents for Parkinson's disease. *Neurobiol. Dis.* **136**, 104712 (2020).
89. Choi, M. et al. Conformation-specific antibodies targeting aggregated forms of α-synuclein block the propagation of synucleinopathy. *Exp. Neurobiol.* **31**, 29–41 (2022).
90. Chen, Y. H. et al. Administration of AAV-alpha synuclein NAC antibody improves locomotor behavior in rats overexpressing alpha synuclein. *Genes* **12**, 948 (2021).
91. Butler, Y. R. et al. α-Synuclein fibril-specific nanobody reduces prion-like α-synuclein spreading in mice. *Nat. Commun.* **13**, 4060 (2022).
92. Fassler, M., Benaim, C. & George, J. A single chain fragment variant binding misfolded alpha-synuclein exhibits neuroprotective and antigen-specific anti-inflammatory properties. *Cells* **11**, 3822 (2022).
93. Roshanbin, S. et al. Reduction of αSyn pathology in a mouse model of PD using a brain-penetrating bispecific antibody. *Pharmaceutics* **14**, 1412 (2022).
94. Danzer, K. M. et al. Different species of α-synuclein oligomers induce calcium influx and seeding. *J. NeuroSci.* **27**, 9220–9232 (2007).
95. Ghee, M., Melki, R., Michot, N. & Mallet, J. PA700, the regulatory complex of the 26S proteasome, interferes with alpha-synuclein assembly. *FEBS J.* **272**, 4023–4033 (2005).
96. Encinas, M. et al. Sequential treatment of SH-SY5Y cells with retinoic acid and brain-derived neurotrophic factor gives rise to fully differentiated, neurotrophic factor-dependent, human neuron-like cells. *J. Neurochem.* **75**, 991–1003 (2000).
97. Neumann, M. et al. Phosphorylation of S409/410 of TDP-43 is a consistent feature in all sporadic and familial forms of TDP-43 proteinopathies. *Acta Neuropathol.* **117**, 137–149 (2009).
98. Strobel, B. et al. Standardized, scalable, and timely flexible adeno-associated virus vector production using frozen high-density HEK-293 cell stocks and CELLdiscs. *Hum. Gene Ther. Method* **30**, 23–33 (2019).
99. Kahle, P. J. et al. Subcellular localization of wild-type and Parkinson's disease-associated mutant alpha-synuclein in human and transgenic mouse brain. *J. Neurosci.* **20**, 6365–6373 (2000).
100. Gentzel, R. C. et al. Intracranial administration of alpha-synuclein fibrils in A30P-synuclein transgenic mice causes robust synucleinopathy and microglial induction. *Neurobiol. Aging* **106**, 12–25 (2021).
101. Zhang, B. et al. Stereotaxic targeting of alpha-synuclein pathology in mouse brain using preformed fibrils. *Methods Mol. Biol.* **1948**, 45–58 (2019).
102. Strobel, B. et al. A small-molecule-responsive riboswitch enables conditional induction of viral vector-mediated gene expression in mice. *ACS Synth. Biol.* **9**, 1292–1305 (2020).

## ACKNOWLEDGEMENTS

The authors would like to acknowledge the expert experimental support from Peter Anding, Sabine Finger, and Monika Palchaudhuri in the initial phases of this project. Funding has been exclusively provided by Boehringer Ingelheim Pharma GmbH & Co KG.

## AUTHOR CONTRIBUTIONS

C.K., T.L., S.L., R.M., M.N., D.W., F.I. and T.C. designed the studies. T.C. wrote the manuscript. M.D., D.B., P.R. and J.S. performed the actual experiments. T.S., M.N. and B.S. analyzed the immunohistopathology.

## COMPETING INTERESTS

None of the authors declare a competing financial or non-financial interest. All authors except M.N., R.M. and J.S. were employed by Boehringer Ingelheim, a privately owned pharmaceutical company, at the time this work was executed. Nobody holds stock or stock options of Boehringer Ingelheim. No patent applications have been filed related to this work.

## ADDITIONAL INFORMATION

**Supplementary information** The online version contains supplementary material available at https://doi.org/10.1038/s41531-023-00542-9.

**Correspondence** and requests for materials should be addressed to Thomas Ciossek.